

# Nuclear Parton Distributions and the Drell-Yan Process

S. A. Kulagin<sup>1,\*</sup> and R. Petti<sup>2,†</sup>

<sup>1</sup>*Institute for Nuclear Research of the Russian Academy of Sciences, Moscow 117312, Russia*

<sup>2</sup>*Department of Physics and Astronomy,  
University of South Carolina, Columbia SC 29208, USA*

## Abstract

We study the nuclear parton distribution functions basing on our recently developed semi-microscopic model, which takes into account a number of nuclear effects including nuclear shadowing, Fermi motion and nuclear binding, nuclear meson-exchange currents and off-shell corrections to bound nucleon distributions. We discuss in details the dependencies of nuclear effects on the type of parton distribution (nuclear sea vs. valence) as well as on the parton flavour (isospin). The resulting nuclear parton distributions are applied to calculate the ratios of cross sections for proton-induced Drell-Yan production off different nuclear targets. We obtain a good agreement on the magnitude, target and projectile  $x$  and the dimuon mass dependence of proton-nucleus Drell-Yan process data from the E772 and E866 experiments at Fermilab.

PACS numbers: 13.60.Hb, 25.30.Mr, 12.38.Qk

Keywords: Deep-inelastic scattering, parton distributions, nuclear parton distributions, EMC effect, Drell-Yan process

---

\* kulagin@ms2.inr.ac.ru

† Roberto.Petti@cern.ch

## I. INTRODUCTION

Relying on the QCD factorization theorem [1], parton distributions (PDFs) determine the leading contributions to the cross sections of various hard processes involving leptons and hadrons. In this context, PDFs are universal process-independent characteristics of the target at high invariant momentum transfer  $Q$ , which are extracted from global fits [2–5] using data on lepton-nucleon deeply-inelastic scattering (DIS), as well as the data on muon pair production in hadron collisions (Drell-Yan reaction, or DY).

Electron and muon DIS experiments off nuclear targets demonstrated significant nuclear effects with a rate that is more than one order of magnitude larger than the ratio of the nuclear binding energy to the nucleon mass [6, 7]. These observations rule out the naive picture of the nucleus as a system of quasi-free nucleons and indicate that the nuclear environment plays an important role even at energies and momenta much higher than those involved in typical nuclear ground state processes [6–9].

A few phenomenological approaches to nuclear parton distributions (nPDFs) are available in literature [10–12]. Typically such analyses assume separate nuclear corrections for each parton distribution, which are extracted from global fits to nuclear data including DIS, DY production, heavy-ion collisions, etc. Although these studies are useful in constraining nuclear effects for different partons, they provide little information about the underlying physics mechanisms responsible for the nuclear corrections. Furthermore, they result in a large number of free parameters, as well as in nuclear correction factors incorporating explicit parameterizations of the nuclear dependence. We also note that the current phenomenology of nuclear effects in neutrino DIS leads to somewhat controversial results. In particular, Ref.[13] obtains significantly different nuclear PDFs from fits to charged-lepton and (anti)neutrino DIS data, thus challenging the QCD factorization theorem [1]. However the analyses of Refs. [12, 14] disagree with this observation.

Here we follow a different approach and study nPDFs using the semi-microscopic model developed in Ref.[15]. The model incorporates a number of nuclear corrections including the smearing with the energy-momentum distribution of bound nucleons (Fermi motion and binding), the off-shell correction to bound nucleon structure functions, the contributions from meson exchange currents and the propagation of the hadronic component of the virtual intermediate boson in the nuclear environment. The model quantitatively explains the

observed  $x$ ,  $Q^2$  and  $A$  dependencies of existing nuclear DIS data on a wide range of targets from the deuteron  $^2\text{H}$  to the lead  $^{207}\text{Pb}$  [15–17].

The model of Ref.[15] accounts for the modification of the PDFs in a bound nucleon through the off-shell dependence of structure functions. In a weakly-bound system this effect is described as a linear correction in the nucleon virtuality  $p^2 - M^2$  with  $p$  the nucleon four-momentum and  $M$  the nucleon mass [22]. The strength of the effect is governed by the relative response of a parton distribution to the variation of the nucleon invariant mass  $p^2$  in the vicinity of the mass shell, which is described by the function  $\delta f$  which depends on Bjorken variable  $x$ . We note that by definition  $\delta f(x)$  describes the nucleon and in a certain sense can be viewed as a new nucleon structure function. Apparently, this function does not contribute to the cross section of the physical nucleon. Instead, it is relevant only for the bound nucleon and describes its response to the interaction with the nuclear medium. The nuclear dependence of this correction is determined by the average nucleon virtuality (off-shellness) in a nucleus. The off-shell correction proved to be an important contribution to the nuclear EMC effect at large  $x$  and was determined phenomenologically from the analysis of data on ratios of DIS structure functions in different nuclei [15]. In a simple single-scale model, in which the quark momentum distributions in the nucleon are functions of the nucleon radius, the observed behaviour of  $\delta f(x)$  can be interpreted in terms of the "swelling" (i.e. increase of the size) of the bound nucleon in the nuclear environment. In particular, the analysis of Ref.[15] suggests that the nucleon core radius increases by about 10% in iron, while this effect is significantly smaller, about 2%, in the deuteron.

Note that Refs. [15–17] assume a universal function  $\delta f(x)$ , which is flavor independent and also isospin blind (i.e. same for proton and neutron). The study of the flavor and isospin dependence of  $\delta f(x)$  requires nuclear data on high-energy processes which can provide a flavor selection, like hadronic DY reaction or (anti)neutrino DIS. In the present study we use data on Drell-Yan production to verify the predictions of the model of Ref.[15] and also to address possible differences in the off-shell correction between valence and sea quark distributions.

At small values of  $x$  nuclear corrections in DIS are dominated by the effects of the propagation of strongly-interacting hadronic states in the nuclear environment [24–26]. Such effects can be described in terms of multiple scattering series [27, 28] in the effective scattering amplitude with the relevant quantum numbers. In this paper we discuss in details how

this coherent nuclear correction depends on the isospin and  $C$ -parity of the (anti)quark distributions.

We emphasize that the nuclear mechanisms listed above give rise to effects located in different kinematical regions of Bjorken  $x$ . For instance, the correction related to the nuclear binding (separation) energy is mostly relevant at large  $x \sim 0.5 - 0.7$  [18, 21–23], while coherent effects related to the propagation of virtual hadronic states are important at small  $x < 0.05$  [24–26]. It is important to realize that these effects, which may appear as unrelated, are actually linked together by the normalization conditions and the energy-momentum sum rules. For instance, the momentum sum rule is known to be a useful tool in predicting the anti-shadowing region in nuclear parton distributions [29, 30]. In this paper we use the normalization conditions for the isoscalar and the isovector valence quark distributions as dynamical equations for the effective scattering amplitudes relevant for the coherent nuclear correction. These equations are then solved in terms of the off-shell function  $\delta f$ , thus providing a relation between the nuclear shadowing and the off-shell effects.

Conventionally, we assume that the relevant nuclear constituents are nucleons interacting via mesonic fields which provide nuclear binding. The nPDFs are then determined by the convolution of light-cone distribution function of bound nucleons with the corresponding nucleon PDFs. The nucleon light-cone distribution functions are driven by the nuclear spectral function, which defines the energy-momentum distribution of bound nucleons [15–22]. The calculation of mesonic correction is less certain and model-dependent [33–41]. However, the nuclear mesonic light-cone distributions are subject to important constraints from the energy-momentum conservation and from the equations of motion connecting the nucleon and the meson correlation functions [21]. In this paper we further discuss the resulting relations for the moments of the nuclear meson light-cone distributions and use them to calculate the mesonic correction to nuclear PDFs.

As an important application of our studies, we present detailed predictions for the nuclear DY reaction. The DY process offers a direct probe of the sea quark content in nucleons and nuclei [45, 46]. The use of DY data in combination with DIS data allows thus a separation of the nuclear corrections for valence and sea quark distributions. The measurements of DY production off nuclear targets by the E772 and E866 experiments [47, 48] at Fermilab do not show any significant enhancement of the sea quark distributions in heavy nuclei for  $0.1 \leq x \leq 0.3$ . Traditionally, this result has been considered in disagreement with

the enhancement of the meson cloud of a bound nucleon, which is in turn related to the nuclear binding [44]. In this paper we revisit the calculation of nuclear sea and valence quark distributions and argue that the enhancement of nuclear antiquarks due to the nuclear meson exchange currents is partially cancelled by a negative shadowing correction. We examine in details the ratios of DY cross sections for different nuclear targets and show that the predicted nPDFs provide a good description of both the magnitude and the  $x$  and mass dependence of the data of Refs.[47, 48].

This article is organized as follows. In Sec.II we review the model of nuclear corrections to PDFs and discuss their dependence on the type of PDFs. In particular, we study in details the nuclear corrections for the isoscalar  $q_0 = u + d$  and isovector  $q_1 = u - d$  distributions, as well as the dependence of nuclear effects on the  $C$  parity of the quark distributions  $q^\pm = q \pm \bar{q}$ . In Sec.III we apply our results to the muon pair production off nuclear targets and provide a detailed comparison of our predictions with the available data [47, 48]. In Sec.IV we discuss and summarize our results.

## II. NUCLEAR PARTON DISTRIBUTION FUNCTIONS

It is well-known that a PDF describes the momentum distribution of the corresponding parton in a target. While this is true in a reference frame in which the target has a large momentum (infinite momentum frame), the interpretation of PDFs in the target rest frame is somewhat more complicated. In the target rest frame a PDF would also depend on the target energy spectrum and it also includes the interaction effects of hadronic component of the virtual photon with the target (see, e.g., [26]). We recall that in the target rest frame the characteristic propagation time (or longitudinal distance) of the hadronic fluctuations of the virtual photon is  $L \sim (Mx)^{-1}$ , where  $M$  the nucleon mass and  $x$  the Bjorken scaling variable [31]. At small  $x$ , where  $L$  is large, diffraction processes dominate the parton distributions. However, when  $L$  becomes comparable to the nucleon size, their contribution is reduced.

The scale  $L$  can be used to roughly identify two different kinematical regions for nuclear effects. At large values of  $x$ , for which  $L < d$  where  $d$  is average distance between bound nucleons, nuclear PDFs can be approximated by the incoherent contributions from bound protons and neutrons. The picture changes at small  $x$  ( $L \gg d$ ), where the effects related to the propagation of the virtual hadronic (or quark-gluon) states in the nuclear medium

introduce essential corrections to the impulse approximation. The interference of multiple scattering contributions and the energy dependence of the corresponding scattering amplitudes can lead to either a negative (shadowing) or a positive (antishadowing) correction, depending on the values of  $x$ . It is worth noting that this correction, in general, is not universal and may depend on the type of the parton distribution, as indicated by the studies of Ref.[15, 16, 32] and also by phenomenology [11–13].

In this article we study the nuclear quark and antiquark distributions (nPDFs). We will use the notation  $q_{f/T}(x, Q^2)$  for the distribution of quarks of the type  $f$  in a target  $T$ . The (anti)quark distribution in a nucleus receives a number of contributions and can be written as [15] (for brevity, we suppress explicit dependencies on  $x$  and  $Q^2$ ):

$$q_{f/A} = q_{f/A}^{\text{IA}} + \delta_{\text{coh}} q_f + \delta_{\pi} q_f, \quad (1)$$

where the first term on the right side is the contribution from bound protons and neutrons in the impulse approximation, and the other terms are the corrections to the impulse approximation due to coherent nuclear interactions of the hadronic component of the virtual photon and to nuclear meson exchange currents. These contributions are reviewed in the following sections.

### A. Impulse Approximation and Off-shell Corrections

It is well known that in the impulse approximation the nPDFs can be written as a convolution of the proton (neutron) distribution of a nucleus with the corresponding quark distribution of a bound proton (neutron). The nuclear convolution is an integration over both the nucleon light-cone momentum  $y$  and the nucleon off-shellness (virtuality)  $\mu^2$ , since parton distributions in a off-shell nucleon generally depend on its virtuality [22]:

$$q_{f/A}^{\text{IA}} = \sum_{\tau=p,n} f_{\tau/A} \otimes q_{f/\tau} = \sum_{\tau=p,n} \int_{x < y} \frac{d\mu^2 dy}{y} f_{\tau/A}(y, \mu^2) q_{f/\tau}\left(\frac{x}{y}, Q^2, \mu^2\right). \quad (2)$$

The proton and the neutron distribution function  $f$  can be written in terms of the corresponding nuclear spectral function  $\mathcal{P}(\mathbf{p}, \varepsilon)$  [15, 21, 22] (for brevity we drop subscripts identifying the proton and the neutron distributions):

$$f(y, \mu^2) = \int [d\mathbf{p}] \left(1 + \frac{p_z}{M}\right) \mathcal{P}(\mathbf{p}, \varepsilon) \delta\left(y - \frac{p_0 + p_z}{M}\right) \delta(\mu^2 - p^2), \quad (3)$$

where the integration  $[dp] = dp_0 d\mathbf{p}/(2\pi)^4$  is performed over the nucleon momentum  $\mathbf{p}$  and energy  $p_0 = M + \varepsilon$ , and  $p^2 = p_0^2 - \mathbf{p}^2$  is invariant mass of off-shell nucleon. We chose a system of coordinates such that the momentum transfer is antiparallel to  $z$  axis. In the derivation of Eq.(2) and Eq.(3) we also assume the kinematics in the Bjorken limit and drop any powers of  $Q^{-2}$ . Note that the Bjorken variable of the target nucleus is defined in terms of the nucleon mass  $M$  and the energy transfer  $q_0$  in the target rest frame as  $x = Q^2/2Mq_0$ . This variable can vary within the interval  $0 < x < M_A/M$ , where  $M_A$  is the mass of a target nucleus.

It should be noted that Eq.(3) was obtained by expanding a general relativistic expression in powers of  $\mathbf{p}/M$  and is valid to order  $\mathbf{p}^2/M^2 \sim |\varepsilon|/M$  (including those terms) [21, 22]. To this order the nuclear structure functions in impulse approximation are determined by nonrelativistic nuclear spectral function which can be written as

$$\mathcal{P}(\mathbf{p}, \varepsilon) = \int dt e^{i\varepsilon t} \langle \psi^\dagger(\mathbf{p}, t) \psi(\mathbf{p}, 0) \rangle, \quad (4)$$

where  $\psi(\mathbf{p}, t)$  is the nonrelativistic nucleon operator in the momentum-time representation (for more details see Ref.[15]). By definition, the spectral function describes the energy-momentum distribution of bound nucleons. Note that  $\varepsilon$  in Eq.(4) includes the recoil kinetic energy of the residual system of  $A - 1$  nucleons, as can be seen after inserting a complete set of states and integrating over the time. The proton (neutron) nuclear spectral function is normalized to the number of protons (neutrons),  $\int [dp] \mathcal{P}_{p(n)} = Z(N)$ . Using Eq.(3) we explicitly verify that the proton and neutron distribution functions are normalized accordingly

$$\int dy d\mu^2 f_{p(n)/A}(y, \mu^2) = Z(N). \quad (5)$$

Equations similar to (1) can be written for the antiquark and gluon distributions in nuclei. The distribution functions are independent of  $Q^2$  in the Bjorken limit and the  $Q^2$  evolution of nuclear PDFs in the impulse approximation is governed by the evolution of the PDFs of the corresponding nuclear constituents. For the discussion of finite  $Q$  corrections to nuclear convolution (2) we refer to Ref.[15] (see also [23] for spin-dependent DIS).

Note that Eq.(2) describes DIS off an off-shell nucleon and for that reason the bound nucleon PDFs depend on the invariant mass  $p^2$  as additional variable. The analysis of the off-shell effect can be significantly simplified by observing that the nucleon virtuality  $v = (p^2 - M^2)/M^2$  is, on average, a small parameter [15]. We can then expand the function

$q(x, Q^2, p^2)$  as a series in  $v$  in the vicinity of the mass shell  $p^2 = M^2$ , keeping only terms up to the one linear in  $v$ :

$$q(x, Q^2, p^2) \approx q(x, Q^2)(1 + \delta f(x, Q^2)v), \quad (6a)$$

$$\delta f(x, Q^2) = \partial \ln q(x, Q^2, p^2) / \partial \ln p^2, \quad (6b)$$

where  $q(x, Q^2)$  is the quark distribution in the on-shell nucleon and the derivative in Eq.(6b) is evaluated at  $p^2 = M^2$ . The magnitude of the off-shell effect is determined by the function  $\delta f$ . This function describes the response of the quark distribution in a nucleon to the modification of its invariant mass due to interaction effects in the vicinity of the mass shell. The function  $\delta f$  was extracted phenomenologically from analysis of data on the nuclear DIS in Ref. [15]. This analysis suggests a common off-shell function for the quark and antiquark distributions, independent of  $Q^2$  and of the parton type. We will further test this assumption by comparing our predictions with data on dimuon pair production in nuclear  $p$ - $A$  reactions in Sec.III.

Note that by the definition the function (6b) describes the properties of the bound nucleon. The hypothesis that  $\delta f$  does not depend on the specific nucleus was verified with a good accuracy for nuclei ranging from  $^{207}\text{Pb}$  down to  $^3\text{He}$  [15, 17]. We found that off-shell correction together with nuclear binding correction is important in the description of the slope and position of the minimum of the ratio of nuclear structure functions (EMC effect). Overall this model has been successfully used to explain the observed  $x$ ,  $Q^2$  and  $A$  dependencies of nuclear DIS data on a wide range of targets from  $^2\text{H}$  to  $^{207}\text{Pb}$  [15–17].

Complex nuclei typically have different numbers of protons and neutrons, and therefore nuclear PDFs can include both isoscalar and isovector components. In order to properly take this effect into account it is convenient to consider the isoscalar  $q_0 = u + d$  and the isovector  $q_1 = u - d$  combinations of quark distributions. Assuming the isospin symmetry of parton distributions, which can be written as  $q_{0/p} = q_{0/n}$  and  $q_{1/p} = -q_{1/n}$ , from Eq.(1) we infer that  $q_0$  and  $q_1$  are governed by the isoscalar and the isovector nucleon distributions, respectively:

$$q_{0/A} = (f_{p/A} + f_{n/A}) \otimes q_{0/p}, \quad (7a)$$

$$q_{1/A} = (f_{p/A} - f_{n/A}) \otimes q_{1/p}, \quad (7b)$$

where we use notations defined in Eq.(2). It should be emphasized that the separations of



distributions with different isospin in Eqs.(7) is due to assumed isospin symmetry between  $u$  and  $d$  quark distributions in the proton and neutron.<sup>1</sup> In the present studies we use the isoscalar and isovector nuclear spectral function of Ref.[15].

The correction driven by the nuclear spectral function (Fermi motion and nuclear binding [18, 21]) along with the off-shell correction [22] are the leading nuclear effects at large  $x$ , as verified by the extensive studies of Refs.[15, 17]. At small  $x$  there are significant corrections to the impulse approximation. It is worth mentioning that in order to satisfy the nuclear light-cone momentum sum rule, contributions from degrees of freedom other than nucleons are required. Indeed, we obtain the fraction of the nuclear light-cone momentum carried by nucleons by integrating the nucleon distribution function:

$$\langle y \rangle_N = \int dy dp^2 f_0(y, p^2) y = 1 + \frac{\langle \varepsilon \rangle + \frac{2}{3} \langle T \rangle}{M}, \quad (8)$$

where the distribution  $f_0 = (f_{p/A} + f_{n/A})/A$  is normalized to unity and  $\langle \varepsilon \rangle$  and  $\langle T \rangle = \langle \mathbf{p}^2 \rangle / 2M$  are the nucleon separation and kinetic energy, respectively, averaged with the nuclear spectral function.<sup>2</sup> The correction to unity in Eq.(8) is negative, suggesting that the impulse approximation violates the nuclear light-cone momentum balance. This violation is not unexpected because the same fields responsible for the nuclear binding also carry the missing light-cone momentum and therefore they should be considered explicitly.

## B. Correction due to Nuclear Meson Exchange Currents

Let us discuss the correction originated from the virtual mesons exchanged between bound nucleons, which was extensively discussed in context of the nuclear EMC effect [33–37, 39]. Following the approach discussed in Sec.II A this correction can be written in terms of the convolution (2) of the nuclear pion distribution function with the (anti)quark distribution in a virtual pion. Pions can be in three possible charge states:  $\pi^0, \pi^+, \pi^-$ . Similarly to Sec.II A, we separate the pion corrections for the isoscalar and the isovector nuclear PDFs. Assuming the isospin symmetry of the quark distributions in different pion states,  $q_{0/\pi^+} = q_{0/\pi^-} = q_{0/\pi^0}$  and  $q_{1/\pi^+} = -q_{1/\pi^-}$  and  $q_{1/\pi^0} = 0$ , we have [15]

$$\delta_\pi q_{0/A}(x, Q^2) = f_{\pi/A} \otimes q_{0/\pi}, \quad (9a)$$

<sup>1</sup> Possible violations of the isospin symmetry in PDFs were discussed in [50].

<sup>2</sup> Note that our definition of  $\varepsilon$  includes the energy of the recoil nucleus such that, e.g., for the deuteron

$\varepsilon = \varepsilon_D - \mathbf{p}^2 / 2M$  with  $\varepsilon_D \approx -2.2$  MeV the deuteron binding energy. See Ref [17] for a discussion about the relation between  $\varepsilon$  and the “conventional” separation energies and spectral functions.

$$\delta_\pi q_{1/A}(x, Q^2) = (f_{\pi^+/A} - f_{\pi^-/A}) \otimes q_{1/\pi^+}. \quad (9b)$$

The pion distribution entering in the first equation,  $f_{\pi/A}$ , is the sum over the pion states  $\pi^+$ ,  $\pi^0$ , and  $\pi^-$ . The pion distributions refer only to the nuclear pion excess, since the scattering off virtual pion emitted and absorbed by the same nucleon (nucleon pion cloud) should be already included into the proton and neutron PDFs.

The isospin symmetry suggests equal distribution of pion quarks and antiquarks in the isoscalar combination, thus  $q_{0/\pi}^- = 0$ . For this reason pion correction to the isoscalar nuclear valence quark distributions vanishes,  $\delta_\pi q_{0/A}^- = 0$ . However, the nuclear sea is obviously affected by the pion contribution. Note that the isovector part of the valence quark distribution  $q_{1/\pi}^-$  is finite. Thus nuclear pions, in general, contribute to the isovector nuclear valence distribution  $q_{1/A}^-$ . This correction is driven by the  $\pi^+ - \pi^-$  asymmetry of the nuclear pion distributions, as it can be seen from Eq.(9). In the present discussion we assume for simplicity identical  $\pi^+$  and  $\pi^-$  nuclear distributions and postpone the discussion of the isovector pion effect for future studies. Thus we also have  $\delta_\pi q_{1/A}^- = 0$ .

The pion light-cone distribution can be written as [15, 21]

$$f_{\pi/A}(y, \mu^2) = 2yM \int [dk] \mathcal{D}_{\pi/A}(k) \delta\left(y - \frac{k_0 + k_z}{M}\right) \delta(\mu^2 - k^2), \quad (10)$$

$$\mathcal{D}_{\pi/A}(k) = \int dt \exp(ik_0 t) \langle \varphi^\dagger(\mathbf{k}, t) \varphi(\mathbf{k}, 0) \rangle, \quad (11)$$

where, similarly to Eq.(4), the averaging is taken over the nuclear ground state and  $\varphi$  is the pion field operator in the momentum-time space.<sup>3</sup> We also assume the sum over different pion isospin states.

The pion energy-momentum distribution  $\mathcal{D}_{\pi/A}(k)$  is proportional to the imaginary part of the full pion propagator in a nucleus, which is, in turn, proportional to the spin-isospin nuclear response function. This relation was exploited in a number of calculations of the nuclear pion/meson correction to nuclear structure functions [34, 37, 39, 41]. These studies show an enhancement of nuclear structure functions in the region  $0.05 < x < 0.15$ . However, it should be noted that the specific results on the nuclear pion distribution are sensitive to the details of the pion-nucleon form-factor, as well as to the treatment of the particle-hole nuclear excitations (i.e. uncertainties in the values and possible energy-momentum dependence of the Landau-Migdal parameters), and  $\Delta$  degrees of freedom in the response function.

---

<sup>3</sup>  $\varphi(\mathbf{k}, t)$  is the Fourier transform of the pion field operator  $\varphi(\mathbf{r}, t)$  in the Heisenberg representation.

We use a different approach [21]. In the following we will discuss the constraints on the pion distribution function which can be derived by considering the requirement of the nuclear light-cone balance and studying the meson contribution to the nuclear potential energy. We will focus on the dependence on the light-cone variable and will not discuss the off-shell effect on the virtual pion PDFs. To this end, we integrate the distribution (10) over the pion virtuality,  $f_{\pi/A}(y) = \int d\mu^2 f_{\pi/A}(y, \mu^2)$ .

Equation(10) defines an antisymmetric function  $f_{\pi/A}(-y) = -f_{\pi/A}(y)$ . This property allows us to derive the sum rules for the odd moments of the pion distribution function in the physical region of  $y > 0$ . We notice that the first moment of (10) reduces to the light-cone component of the pion energy-momentum tensor  $\theta_{++}^\pi = (\partial_0\varphi)^2 + (\partial_z\varphi)^2$  in a nucleus

$$\langle y \rangle_\pi = \int dy y f_{\pi/A}(y) = \langle \theta_{++}^\pi \rangle / M. \quad (12)$$

It was shown in Ref.[21] that the nucleon and the pion distribution functions (3,10) are consistent with the light-cone momentum balance equation

$$\langle y \rangle_\pi + \langle y \rangle_N = M_A / (AM), \quad (13)$$

where  $M_A = A(M + \varepsilon_B)$  is the nucleus mass and  $\varepsilon_B$  is the nuclear binding energy per nucleon.

In order to further constrain the pion distribution (10), we consider the average  $y^{-1}$ , which is proportional to  $\varphi^2$  averaged over the nuclear ground state [21]

$$\langle y^{-1} \rangle_\pi = \int dy y^{-1} f_{\pi/A}(y) = M \langle \varphi^2 \rangle. \quad (14)$$

A number of constraints on the nuclear pion distribution  $\mathcal{D}_{\pi/A}(k)$  can be obtained in a model with a nuclear Hamiltonian including nucleons interacting with the pion field. Consider the pion kinetic term in the nuclear Hamiltonian. Its mean value over the nuclear ground state can be written as

$$\langle (\nabla\varphi)^2 + m_\pi^2 \varphi^2 \rangle = -\langle V_\pi \rangle, \quad (15)$$

where  $\langle V_\pi \rangle$  is the contribution to the nuclear potential energy due to the one-pion exchange potential, averaged over the nuclear ground state. This relation can be derived by using the equation of motion for the pion field operator in the static approximation  $\partial_0\varphi = 0$  [21]. We comment in this context that the pion field in nuclei is generated by nucleon sources and

its time dependence describes retardation effects in the nucleon–nucleon interaction. In a nonrelativistic system this effect is small since typical energy variations are small compared to the pion mass. In the same approximation, for the pion energy-momentum tensor we have  $\langle \theta_{++}^\pi \rangle = \frac{1}{3} \langle (\nabla \varphi)^2 \rangle$ . Using this relation in Eqs. (12) and (15) we obtain

$$\langle (\nabla \varphi)^2 \rangle = 3M \langle y \rangle_\pi, \quad (16a)$$

$$m_\pi^2 \langle \varphi^2 \rangle = -\langle V_\pi \rangle - 3M \langle y \rangle_\pi. \quad (16b)$$

It is interesting to note that the normalization of the pion distribution (10), i.e. the average pion excess number in a nucleus, can be constrained in terms of the moments  $\langle y \rangle_\pi$  and  $\langle y^{-1} \rangle_\pi$ . Indeed, assuming  $f_{\pi/A} \geq 0$ , we apply the triangle inequality to the distribution (10) and obtain

$$N_\pi = \int dy f_{\pi/A}(y) < (\langle y \rangle_\pi \langle y^{-1} \rangle_\pi)^{1/2}. \quad (17)$$

At this point it should be noted that the pion exchange alone is not sufficient to describe the nucleon-nucleon interaction. Other mesons, such as scalar  $\sigma$ , vector  $\omega$  and  $\rho$ , contribute to both the nucleon-nucleon interaction and the nuclear DIS. Their contribution to the nuclear parton distribution is described by equations similar to Eqs. (10) and (11), with the pion field replaced by the corresponding mesonic field. The light-cone balance equation (13) and the pion contribution to nuclear potential energy in Eq.(15) can be generalized to include other mesonic contributions. Let us consider the light-cone distribution function corresponding to the sum of  $\pi$ ,  $\rho$ ,  $\omega$  and  $\sigma$  mesons:

$$f_M(y) = \sum_{m=\pi,\rho,\dots} f_m(y) \quad (18)$$

The moments of this distribution can be written similarly to Eqs. (12) and (14) as

$$\langle y \rangle_M = \frac{1}{3M} \sum_m \langle (\nabla \phi_m)^2 \rangle, \quad (19)$$

$$\langle y^{-1} \rangle_M = M \sum_m \langle \phi_m^2 \rangle, \quad (20)$$

where for the (pseudo)scalar mesons  $\phi_m^2$  is the corresponding meson field squared, and for the vector mesons we have  $\phi_\omega^2 = \boldsymbol{\omega}^2 - \omega_0^2$  and a similar term for the  $\rho$  meson.

The generalization of the light-cone balance equation is straightforward, since Eq.(13) holds in the presence of several meson fields, with  $\langle y_\pi \rangle$  replaced with the total meson light-cone momentum  $\langle y_M \rangle$ . The pion energy equation (15) can also be generalized for the presence

of several meson fields

$$\sum_m \langle (\nabla \phi_m)^2 + m_m^2 \phi_m^2 \rangle = -\langle V \rangle, \quad (21)$$

where  $m_m$  is the mass of the corresponding meson. In the r.h.s. of Eq.(21) the term  $\langle V \rangle$  is the nuclear potential energy, i.e. the full one-meson-exchange potential  $V = V_\pi + V_\omega + V_\rho + V_\sigma$  averaged over the nuclear ground state. The nuclear potential energy  $\langle V \rangle$  is related to the mean separation and kinetic energy as (see Sec.3 of Ref.[21] for more detail)

$$\langle \varepsilon \rangle = \langle T \rangle + \langle V \rangle \quad (22)$$

Using Eqs. (19) and (21) we can estimate the average  $\phi_m^2$ , which determines the moment  $\langle y^{-1} \rangle_M$ :

$$m_M^2 \sum_m \langle \phi_m^2 \rangle = -\langle V \rangle - 3M \langle y \rangle_M, \quad (23)$$

where  $m_M$  is an average meson mass.

We use the constraints and equations discussed above to model the nuclear meson distribution (10). It is important to note that Eqs.(19) through (23) allow us to constrain the overall behavior of the meson distribution in terms of the nucleon spectral function (4), the energy parameters  $\langle \varepsilon \rangle$  and  $\langle T \rangle$ . We must consider a realistic parameterization of the distribution (10). We first note that Eq.(10) shows a linear dependence on  $y$  as  $y \rightarrow 0$ . The distribution (10) is concentrated mainly in the region  $y \sim k_M/M$  where  $k_M$  is a typical virtual meson momentum which can be estimated as

$$k_M^2 = \sum_m \langle (\nabla \varphi_m)^2 \rangle / \sum_m \langle \varphi_m^2 \rangle = 3M^2 \langle y \rangle_M / \langle y^{-1} \rangle_M. \quad (24)$$

Note that this equation gives the average pion momentum in terms of the moments  $\langle y \rangle_M$  and  $\langle y^{-1} \rangle_M$  of the light-cone distribution (18). Using Eqs.(19) through (23) and  $\langle \varepsilon \rangle$  and  $\langle T \rangle$  calculated with the spectral function of Ref.[15], we obtain  $\langle y \rangle_M = 0.023$  and  $\langle y^{-1} \rangle_M = 0.954$  for iron, while for the deuteron we obtain 0.0045 and 0.402, respectively. These values suggest that the characteristic value of  $y \sim k_M/M$  spans the region 0.2 – 0.3 for light and heavy nuclei. The region  $y \sim 1$  requires relativistic momenta of virtual mesons  $\sim 1$  GeV, which we assume to be suppressed. On the basis of these arguments, we consider the following model for the meson distribution in the region  $0 < y < 1$

$$f_{M/A}(y) = c y(1-y)^n. \quad (25)$$

The parameters  $c$  and  $n$  are fixed from  $\langle y \rangle_M$  and  $\langle y^{-1} \rangle_M$ . By integrating Eq.(25) we obtain an average meson number  $N_M = 0.11$  for the iron nucleus and 0.031 for the deuteron.

### C. Effects due to propagation of intermediate hadronic states

In this section we review corrections arising due to the propagation of the hadronic component of the intermediate boson in the nucleus rest frame. These effects are relevant at low values of Bjorken  $x$ , as the virtual hadronic states have an average lifetime (or the correlation length)  $L \sim (Mx)^{-1}$  [31]. For the leading contribution to the DIS structure functions the coherent multiple scattering interactions of intermediate states with nucleons lead to a negative correction known as nuclear shadowing effect, as discussed in a number of studies (for a review see Ref.[26]).

We follow the approach developed earlier for the structure functions in Refs.[15, 16] and evaluate this correction to nuclear PDFs. We will approximate the sum over the set of intermediate hadronic states by a single effective state and describe its interaction with the nucleon by effective scattering amplitude  $a$ . Let  $a_{qp}$  and  $a_{\bar{q}p}$  be the effective proton scattering amplitude of this state corresponding to the quark and antiquark distributions of type  $q$  in the proton. Similar notations will be used for the neutron distributions. The ratio  $\delta\mathcal{R} = \delta_{\text{coh}}q_N/q_N^{\text{coh}}$  describes the relative nuclear effect in the coherent component of the quark distribution. Using the optical theorem this ratio can be written in terms of effective cross sections or the imaginary part of effective amplitudes in the forward direction

$$\delta\mathcal{R}_f = \text{Im } \mathcal{T}^A(a_f)/(A \text{Im } a_f) \quad (26)$$

where  $\mathcal{T}^A(a)$  is the sum of nuclear multiple-scattering series driven by the propagation of the intermediate hadronic states in a nucleus. Note that the multiple scattering series should start from the double scattering term, as the single scattering term is already accounted in the impulse approximation of Eq.(1). The elastic scattering amplitude  $a(s, k)$  depends on the center-of-mass energy  $s$  and the momentum transfer  $k$ . We choose a normalization of the amplitude such that the optical theorem reads  $\text{Im } a(s, 0) = \sigma(s)/2$ , where  $\sigma$  is the total cross section, and write the amplitude as  $a = (i + \alpha)(\sigma/2) \exp(-Bk^2/2)$ , where the exponent describes the dependence on the momentum transfer.

For the deuteron we only have a double scattering term and the amplitude  $\mathcal{T}^D$  can be

written as

$$\mathcal{T}_D = ia_p(0)a_n(0) \int \frac{d^2k_\perp}{(2\pi)^2} S_D(k_\perp, k_z) e^{-B(k_\perp^2 + k_z^2)}, \quad (27)$$

$$S_D(k) = \int d^3r e^{i\mathbf{k} \cdot \mathbf{r}} |\Psi_D(\mathbf{r})|^2, \quad (28)$$

where  $\Psi_D$  is the deuteron wave function,  $S_D(k)$  is the deuteron elastic form factor, and  $a_{p(n)}(0)$  denotes the proton (neutron) scattering amplitude in the forward direction. Equation (27) is similar to the well-known Glauber formula [27]. However we should note the dependence on the longitudinal momentum transfer  $k_z$ , which is not present in [27]. The longitudinal momentum transfer  $k_z$  develops because of inelastic transitions and depends on the mass of the states produced diffractively [28]. We set  $k_z = Mx$  to account for a finite longitudinal correlation length of the hadronic component of the intermediate boson at high  $Q^2$ .

For heavy nuclei the double scattering term has a form similar to Eq.(27) in the optical approximation

$$\mathcal{T}_A^{(2)}(a) = \frac{i}{2}(1 - A^{-1}) \int \frac{d^2k_\perp}{(2\pi)^2} a(k)S(k)a(-k)S(-k), \quad (29)$$

$$S(k) = \int d^3\mathbf{r} \exp(i\mathbf{k} \cdot \mathbf{r}) \rho(\mathbf{r}), \quad (30)$$

where  $\rho$  is the nuclear density (normalized to the number of particles) and  $aS = a_p S_p + a_n S_n$  is the sum of the proton and the neutron terms with the corresponding density distributions. We note that Eq.(29) holds for a generic nucleus of  $Z$  protons and  $N$  neutrons and thus it accounts for both the isoscalar and the isovector effects in the nuclear shadowing correction. We will discuss the separation of these effects later in this section.

For heavy nuclei the multiple scattering series goes beyond the double scattering term (although the double scattering correction dominates if the mean free path of the hadronic state is larger than the nuclear radius,  $(\rho\sigma)^{-1} > R_A$ ). The sum of the Glauber multiple-scattering series can be written in a compact form for a  $A \gg 1$  nucleus in the optical approximation (see, e.g., Ref.[24])

$$\mathcal{T}^A(a) = i \int_{z_1 < z_2} d^2\mathbf{b} dz_1 dz_2 a\rho^B(\mathbf{b}, z_1)a\rho^B(\mathbf{b}, z_2) e^{i \int_{z_1}^{z_2} dz' a\rho^B(\mathbf{b}, z')} e^{ik_z(z_1 - z_2) - Bk_z^2}, \quad (31)$$

where the integration is performed along the collision axis, chosen to be the  $z$ -axis, and over the transverse positions of the nucleons (impact parameter  $\mathbf{b}$ ),  $a\rho^B = a_p(0)\rho_p^B + a_n(0)\rho_n^B$

with  $\rho_p^B$  and  $\rho_n^B$  the proton and the neutron density convoluted with the profile function of the scattering amplitude in the impact parameter space:

$$\rho^B(\mathbf{b}, z) = \int d^2\mathbf{b}' \frac{\exp(-\frac{(\mathbf{b}-\mathbf{b}')^2}{2B})}{2\pi B} \rho(\mathbf{b}', z) \quad (32)$$

In Eqs. (31) and (32) we use the  $\exp(-Bk^2/2)$  momentum transfer dependence of the scattering amplitude. Note that the proton and the neutron densities are normalized to the proton ( $Z$ ) and the neutron ( $N$ ) numbers, respectively. The density in the exponential factor of Eq.(31) accounts for multiple scattering effects (i.e. triple and higher order rescattering). Equation(31) reduces to Eq.(29) in the double scattering approximation, up to a  $1/A$  term.

We now separate the isoscalar and isovector contributions in Eq.(31), relevant for the  $u$  and  $d$  quark distributions. To this end, we assume the isospin symmetry for the scattering off protons and neutrons, i.e.  $a_{up} = a_{dn}$  and  $a_{dp} = a_{un}$ , and write the amplitudes as  $a_{up} = a_0 + \frac{1}{2}a_1$  and  $a_{dp} = a_0 - \frac{1}{2}a_1$ , where  $a_0$  and  $a_1$  are the isoscalar and isovector amplitudes, respectively. To the first order in  $\beta$  we have [16]:

$$\mathcal{T}^A(a_{u,d}) = \mathcal{T}^A(a_0) \pm \frac{1}{2}\beta a_1 \mathcal{T}_1^A(a_0), \quad (33)$$

where  $+$  should be taken for  $u$  quark, and  $-$  for  $d$  quark, and  $\mathcal{T}_1^A(a) = \partial\mathcal{T}^A(a)/\partial a$ . The first and the second terms in Eq.(33) determine the corrections to the isoscalar and the isovector quark distributions, respectively.

An equation similar to Eq.(33) can be obtained for the antiquark amplitudes. It is convenient to discuss combinations of PDFs with definite isospin and  $C$ -parity. We define  $q_I^\pm = q_I \pm \bar{q}_I$  with  $I = 0, 1$  and combine the quark and antiquark amplitudes in order to derive the nuclear corrections to these PDFs in terms of the ratios  $\delta\mathcal{R}_I^C = \delta_{\text{coh}} q_I^C / (A q_{I/p}^C)$  (note that  $q_{I/p}^C$  are the proton PDFs). We first consider the isoscalar  $I = 0$  case. For coherent nuclear corrections to the  $C$ -even and  $C$ -odd quark distributions we have

$$\delta\mathcal{R}_0^+ = \text{Im} \mathcal{T}^A(a_0^+) / (A \text{Im} a_0^+), \quad (34a)$$

$$\delta\mathcal{R}_0^- = \text{Im}[a_0^- \mathcal{T}_1^A(a_0^+)] / (A \text{Im} a_0^-), \quad (34b)$$

where  $a_0^\pm = a_0 \pm \bar{a}_0$  are the isospin 0 amplitudes with  $C$ -parity  $C = \pm 1$ . We note that Eqs.(34) were obtained by treating the  $C$ -odd amplitude as a small parameter and expanding the difference between the quark and antiquark nuclear amplitudes in series of  $a_0^-$  to the



order  $(a_0^-)^2$  [16]. The effective expansion parameter in Eqs.(34) is the ratio of the amplitudes  $a_0^-/a_0^+$ . The smallness of this parameter can be justified within the Regge pole model of high-energy scattering amplitudes. Indeed, the Pomeron gives the leading contribution to the  $C$ -even amplitude  $a_0^+$ . However, its contribution cancels out in the  $C$ -odd amplitude  $a_0^-$ , which is determined by subleading Regge poles.

It should be noted that the  $C$ -odd ratio  $\mathcal{R}_0^-$  from Eq.(34b) is independent of the  $C$ -odd cross section  $\sigma_0^-$ , but depends on the ratio  $\alpha_0^- = \text{Re } a_0^- / \text{Im } a_0^-$  and on the  $C$ -even cross section, which determines the rate of nuclear effects for parton distributions. The result is also affected by the interference of the real parts of the amplitudes in the  $C$ -even and  $C$ -odd channels. It is interesting to note that we obtain a simple relation between  $\mathcal{R}_0^+$  and  $\mathcal{R}_0^-$  if we only consider the double scattering term in Eqs.(34). We have [15]

$$\frac{\delta\mathcal{R}_0^-}{\delta\mathcal{R}_0^+} = 2 \frac{1 - \alpha_0^- \alpha_0^+}{1 - \alpha_0^{+2}} \quad (35)$$

This equation suggests that the relative nuclear effect for the  $C$ -even and the  $C$ -odd cross sections is independent of the cross section and only depends on the Re/Im ratios of the amplitudes.<sup>4</sup> In case of vanishing  $\alpha_0^+$  the relative  $C$ -odd shadowing effect is enhanced by a factor of 2 [32].

We now discuss the isovector coherent (shadowing) correction to the nuclear (anti)quark distributions. To this end, we consider the multiple scattering corrections to the  $C$ -even and  $C$ -odd isovector combination  $a_u - a_d$  using Eq.(33). Similarly to the isoscalar case discussed above, we expand the terms  $\mathcal{T}_1^A(a_0^+ \pm \frac{1}{2}a_0^-)$  in Eq.(33) in series of  $a_0^-$ . To the first order we obtain

$$\delta\mathcal{R}_1^+ = \beta \text{Im} \left[ a_1^+ \mathcal{T}_1^A(a_0^+) + \frac{1}{4} a_1^- a_0^- \mathcal{T}_2^A(a_0^+) \right] / (A \text{Im } a_1^+), \quad (36a)$$

$$\delta\mathcal{R}_1^- = \beta \text{Im} \left[ a_1^- \mathcal{T}_1^A(a_0^+) + a_1^+ a_0^- \mathcal{T}_2^A(a_0^+) \right] / (A \text{Im } a_1^-), \quad (36b)$$

where  $\mathcal{T}_2(a) = \partial\mathcal{T}_1(a)/\partial a$ .

The corresponding individual corrections for  $u$  and  $d$  quarks and antiquarks are given in terms of the isoscalar ( $q_{0/p} = u + d$ ) and the isovector ( $q_{1/p} = u - d$ ) components of the quark distributions in the proton and  $\delta\mathcal{R}_{0,1}^\pm$  as follows

$$\delta\mathcal{R}_{u,d} = \delta\mathcal{R}_0^+ + \frac{q_0^-}{2q_0} (\delta\mathcal{R}_0^- - \delta\mathcal{R}_0^+) \pm \left[ \frac{q_1}{q_0} \delta\mathcal{R}_1^+ + \frac{q_1^-}{2q_0} (\delta\mathcal{R}_1^- - \delta\mathcal{R}_1^+) \right], \quad (37a)$$

---

<sup>4</sup> Eq.(35) holds at small  $x$  at which the phase  $\exp(ik_z(z_1 - z_2))$  in Eq.(31) can be neglected.

$$\delta\mathcal{R}_{\bar{u},\bar{d}} = \delta\mathcal{R}_0^+ - \frac{q_0^-}{2\bar{q}_0} (\delta\mathcal{R}_0^- - \delta\mathcal{R}_0^+) \pm \left[ \frac{\bar{q}_1}{\bar{q}_0} \delta\mathcal{R}_1^+ - \frac{q_1^-}{2\bar{q}_0} (\delta\mathcal{R}_1^- - \delta\mathcal{R}_1^+) \right], \quad (37b)$$

where the sign  $+$  should be taken for  $u$  quarks, and the sign  $-$  for  $d$  quarks. We recall that  $q_{0,1} = u \pm d$ ,  $\bar{q}_{0,1} = \bar{u} \pm \bar{d}$ , and  $q_{0,1}^- = u_{\text{val}} \pm d_{\text{val}}$  are the (anti)quark distributions for the proton taken for the given  $x$  and  $Q^2$ .

The effective amplitudes  $a$  with either isospin 1 or  $C = -1$  are generally significantly smaller than the leading amplitude  $a_0^+$ , which drives multiple scattering corrections for all distributions, as we can see from Eqs. (34) and (36). If only linear terms in  $a_0^-$  and  $a_1^\pm$  are retained, then the corresponding nuclear ratios depend on the  $\alpha = \text{Re } a / \text{Im } a$  ratios of these amplitudes.

#### D. Normalization Constraints

The PDFs obey a number of sum rules reflecting the general symmetries of the strong interaction. Important examples include the valence quark number sum rule, both for the isoscalar and the isovector channels, and the light-cone momentum sum rule. Because of the underlying symmetries, these sum rules should not be affected by strong interaction including of course the nuclear effects. Therefore, for any particular model it is important to explicitly verify that a cancellation of different nuclear effects occurs in the PDFs sum rules.

We first consider the sum rule of the isoscalar valence quark number per one bound nucleon:

$$N_{\text{val}}^A = A^{-1} \int_0^A dx q_{0/A}^- = 3, \quad (38)$$

where  $q_0^- = u^- + d^-$  is the isoscalar valence quark distribution<sup>5</sup>. We consider now the contributions to Eq.(38) from the various nuclear effects present in our model. First we explicitly calculate the normalization in the impulse approximation by Eq.(2) and obtain

$$N_{\text{val}}^{\text{IA}} = 3 + \delta N_{\text{val}}^{\text{OS}}, \quad (39)$$

$$\delta N_{\text{val}}^{\text{OS}} = \langle v \rangle_0 \int_0^1 dx q_{0/N}^-(x) \delta f(x), \quad (40)$$

---

<sup>5</sup> We do not consider the  $s^-$  and  $c^-$  quark distributions. In general  $s^-(x) \neq 0$ , but this gives vanishing contribution to Eq.(38).

where  $N_{\text{val}}^N = 3$  is the valence quark number in the nucleon,  $\langle v \rangle_0 = \langle p^2 - M^2 \rangle / M^2$  is the nucleon virtuality averaged with the nuclear spectral function (the subscript 0 indicates that we should take the isoscalar part), and  $\delta f$  is the off-shell function defined in Eq.(6b). Note that in the absence of the off-shell correction ( $\delta f = 0$ ) Eq.(38) gives the correct normalization since nuclear effects due to the nuclear spectral function cancel out in the valence quark normalization. The off-shell (OS) correction, in general, does not vanish. As discussed in Sec.II A we assume a single flavor-independent off-shell function  $\delta f(x)$ , common to quark and antiquark distributions. This assumption is supported by the analysis of Ref.[15], which allowed a precise determination of this correction from the measured ratios of structure functions in nuclear DIS. In Sec.III we further verify the universality of  $\delta f$  for all partons by studying the nuclear Drell-Yan process.

The nuclear meson correction to the nuclear valence distribution cancels out (Sec.II B). However, the nuclear coherent (coh) effects give a nonzero contribution to the valence quark normalization:

$$\delta N_{\text{val}}^{\text{coh}} = \int_0^1 dx q_{0/N}^-(x) \delta \mathcal{R}_0^-, \quad (41)$$

where  $\delta \mathcal{R}_0^-$  is given by Eq.(34b). In order to satisfy Eq.(38) we require a cancellation between the off-shell and the coherent corrections in the valence quark normalization:

$$\delta N_{\text{val}}^{\text{OS}} + \delta N_{\text{val}}^{\text{coh}} = 0. \quad (42)$$

It is worth noting that the nuclear (anti)shadowing correction is an effect related to small  $x$  values, while the off-shell correction is mainly located at large  $x$ . Therefore, the normalization constraint introduced by Eq.(42) provides a nontrivial connection between nuclear effects of completely different origin. In the present analysis we use the off-shell function  $\delta f(x)$  of Ref.[15] to calculate the off-shell correction to the normalization  $\delta N_{\text{val}}^{\text{OS}}$ . We then use Eq.(42) in order to constrain the effective amplitudes  $a_0^+$  and  $a_0^-$  in the region of high  $Q^2$ . To this end, we note that in Eq.(34b) the relevant correction  $\delta \mathcal{R}_0^-$  depends on the  $C$ -even cross section  $\sigma_0^+ = 2 \text{Im } a_0^+$  and the phases  $\alpha = \text{Re } a / \text{Im } a$ , both  $C$ -even and  $C$ -odd, responsible for the interference effects in the multiple scattering series. For simplicity we assume that the effective cross section  $\sigma_0^+$  and the phases  $\alpha_i^c$  are independent of energy in the high-energy region, corresponding to small  $x$ , and we fix  $\alpha_0^+ = -0.2$  using the results of Ref.[15]. From Eq.(42) we calculate  $\sigma_0^+(Q^2, \alpha)$  as a function of  $Q^2$  and the  $C$ -odd phase  $\alpha = \alpha_0^-$ . Note that the phase  $\alpha_0^-$  is not directly constrained by Eq.(42). We will determine

this parameter by requiring  $\sigma_0^+(Q^2, \alpha)$  to match the corresponding phenomenological cross section of Ref.[15] in the region of  $15 \lesssim Q^2 \lesssim 20 \text{ GeV}^2$ .<sup>6</sup> We obtain  $\alpha_0^- = 1.41$  and the cross section  $\sigma_0^+$  shown in Fig. 1, together with the phenomenological cross section of Ref.[15] extracted from the analysis of nuclear shadowing data with  $Q^2 \lesssim 20 \text{ GeV}^2$ . The  $1\sigma$  error band for the effective cross-section  $\sigma_0$  shown in Fig. 1 reflects the uncertainty on the off-shell function  $\delta f$  (see the analysis of Ref. [15]).

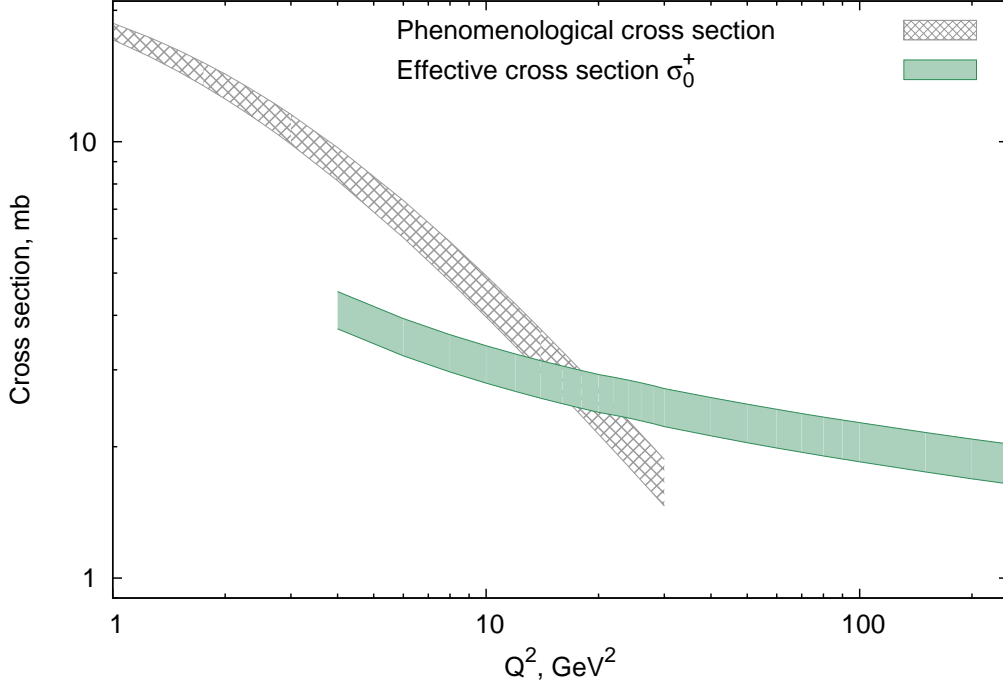


FIG. 1. Effective cross-section  $\sigma_0^+$  extracted from the normalization condition (42) (see text) as a function of  $Q^2$ . The phenomenological cross section of Ref.[15] is also shown for comparison.

We now discuss the normalization of the isovector valence quark distribution. The cancellation of nuclear effects for this quantity is driven by the conservation of the vector current (CVC) and the corresponding sum rule reads

$$N_1^A = A^{-1} \int_0^A dx q_{1/A}^- = \beta \quad (43)$$

where  $q_1^- = u^- - d^-$  and  $\beta = (Z - N)/A$ . This sum rule becomes trivial for an isoscalar nucleus with  $N_1^A = 0$ .

<sup>6</sup> This choice is motivated by the fact that we need values of  $Q^2$  which are sufficiently large to suppress higher-twist contributions, but at the same time which are still in a kinematic region constrained by the available data on nuclear shadowing.

Similarly to the isoscalar case discussed above, we find that the corrections due to nuclear binding and Fermi motion cancel out in Eq.(43), while both, the corrections due to the off-shell effect and coherent multiple scattering, remain finite:

$$\delta N_1^{\text{OS}} = \beta \langle v \rangle_1 \int_0^1 dx q_{1/p}^-(x) \delta f(x), \quad (44)$$

$$\delta N_1^{\text{coh}} = \int_0^1 dx q_{1/p}^-(x) \delta \mathcal{R}_1^-, \quad (45)$$

where  $\langle v \rangle_1 = \langle p^2 - M^2 \rangle_1 / M^2$  is the nucleon virtuality averaged with the isovector nuclear spectral function and  $\delta \mathcal{R}_1^-$  is the coherent nuclear correction to the isovector valence quark distribution given by Eq.(36b).

In order to fulfill the normalization condition given by Eq.(43) for a non-isoscalar nucleus with  $\beta \neq 0$ , we require an exact cancellation between the off-shell and the coherent nuclear correction:

$$N_1^{\text{OS}} + N_1^{\text{coh}} = 0. \quad (46)$$

Similarly to the isoscalar case in Eq.(42), we use Eq.(46) to constrain the unknown amplitude  $a_1^-$  in the isovector channel. Using Eq.(36b) we observe that the isovector coherent correction  $\delta \mathcal{R}_1^-$  is driven by the isoscalar cross section  $\sigma_0^+$  and by the interference of the phases  $\alpha_0^+$  and  $\alpha_1^-$ . We use the isovector spectral function of Ref.[15] in order to calculate  $N_1^{\text{OS}}$  and then obtain  $\sigma_0^+(Q^2, \alpha_1^-)$  by solving Eq.(46). Then we verify that both solutions, the solution to Eq.(42) and that to Eq.(46), agree withing  $1\sigma$  error band for all values of  $Q^2 > 4 \text{ GeV}^2$  at  $\alpha_1^- = 1.73$ .

In order to constrain the amplitude  $a_1^+$  (the parameter  $\alpha_1^+$ ) we use equation similar to Eq.(46) with  $q_1^-$  distribution replaced with  $q_1^+$  and similar procedure. We find  $\alpha_1^+ = 1.46$ .

### E. Light-cone momentum sum rule

Energy-momentum conservation causes the light-cone momentum sum rule on two different levels. On the hadronic level, the nuclear light-cone momentum is shared between nucleons and mesons and we have Eq.(13). On the partonic level the light-cone momentum is balanced between quarks, antiquarks and gluons

$$x_{q/A} + x_{\bar{q}/A} + x_{g/A} = M_A/AM, \quad (47)$$

where the sum over different quark flavors is assumed and  $x_{a/A} = \int_0^{M_A/A} dx x q_{a/A}(x, Q^2)/A$  for the quark distribution of flavour  $a$ , and similar equations for antiquarks and gluons. We recall that the Bjorken variable is defined as  $x = Q^2/(2Mq_0)$ , where  $M$  is the mass of isoscalar nucleon and  $q_0$  is taken in the target rest frame. For the proton (neutron) target we surely have 1 in the right side of Eq.(47) (neglecting a small difference in the proton and neutron masses). Note that Eq.(47) involves the C-even and the isoscalar combination of quark distributions. Using the notation  $x_a^+ = x_a + x_{\bar{a}}$  we have

$$x_{a/A}^+ = \langle y \rangle_N x_{a/N}^+ + \delta^{\text{OS}} x_a^+ + \delta^{\text{mes}} x_a^+ + \delta^{\text{coh}} x_a^+, \quad (48)$$

where the first term on the right is the IA contribution with  $\langle y \rangle_N$  the nucleon fraction of the nuclear light-cone momentum by Eq.(8) and  $x_{a/N}^+$  the corresponding momentum of the nucleon. The correction terms are due to off-shell, MEC and nuclear shadowing effects which read as follows:

$$\delta^{\text{OS}} x_a^+ = \langle y \rangle_N \langle v \rangle_0 \int_0^1 dx x q_{a/N}^+(x, Q^2) \delta f(x), \quad (49a)$$

$$\delta^{\text{mes}} x_a^+ = \langle y \rangle_M x_{a/M}^+, \quad (49b)$$

$$\delta^{\text{coh}} x_a^+ = \int_0^1 dx x q_{a/N}^+(x, Q^2) \delta \mathcal{R}_0^+, \quad (49c)$$

where  $\langle y \rangle_M$  is the meson fraction of the nuclear light-cone momentum by Eq.(19) and  $x_{a/M}^+$  is mean momentum of C-even quark distribution in mesons. These corrections for a number of nuclei are summarized in Table I, in which we display the relative values  $\delta x^+/x_N^+$  for each of the terms in Eqs.(49), and  $x_N^+$  is the total  $q + \bar{q}$  momentum of the proton. Also shown is the gluon fraction  $x_g$  calculated from Eq.(47). The results of Table I were obtained assuming the relative shadowing correction  $\delta \mathcal{R}^+$  is similar for light and heavy quarks. We observe a partial cancellation between different nuclear corrections in the total quark momentum  $x_{q/A}^+$ . The resulting nuclear correction to average  $x^+$  turns out to be significantly smaller than the amplitude of the corresponding correction to the quark distributions in different regions of  $x$  (see Sec.IIF for more details).

The sum rule (47) allows us to evaluate the average nuclear gluon momentum as  $x_{g/A} = M_A/AM - x_{q/A}^+$ . The results shown in Table I indicate the enhancement of gluons in heavy nuclei. In terms of average  $x$  the gluon enhancement is about 1.5 – 2% at  $Q^2 = 20 \text{ GeV}^2$ . The enhancement of nuclear gluon momentum also suggests a gluon antishadowing in nuclei

at large values of  $x$ , in order to compensate the nuclear gluon shadowing effect at small  $x$  [30].

We also found that the ratio  $x_{q/A}^+/x_{q/N}^+$  gradually increases with  $Q^2$  that is explained by decreasing fraction of the (negative) nuclear shadowing correction in the numerator. Then, as it follows from Eq.(47), the gluon ratio  $x_{g/A}/x_{g/N}$  decreases with  $Q^2$ . This in turn may indicate the increasing with  $Q^2$  nuclear shadowing effect for gluons. Detailed discussion of nuclear effects in gluon distribution goes beyond the scope of the present paper and will be addressed elsewhere.

Nucleus	$\langle y \rangle_N$	$\delta^{\text{OS}} x^+/x_N^+$	$\delta^{\text{mes}} x^+/x_N^+$	$\delta^{\text{coh}} x^+/x_N^+$	$x_{q/A}^+/x_{q/N}^+$	$x_{g/A}/x_{g/N}$
$^2\text{H}$	0.9943	0.0058	0.0030	-0.0027	1.0004	0.9974
$^{12}\text{C}$	0.9718	0.0205	0.0127	-0.0217	0.9833	1.0005
$^{56}\text{Fe}$	0.9656	0.0224	0.0148	-0.0336	0.9691	1.0104
$^{119}\text{Sn}$	0.9638	0.0237	0.0156	-0.0403	0.9628	1.0164
$^{184}\text{W}$	0.9626	0.0250	0.0163	-0.0442	0.9596	1.0197

TABLE I. Different contributions to nuclear light-cone momentum sum rule calculated for a few different nuclear targets using the PDF set of Ref.[42, 43] at  $Q^2 = 20 \text{ GeV}^2$ . The last two columns show the nuclear  $q + \bar{q}$  and the gluon  $x$  relative to corresponding nucleon quantities.

## F. Nuclear Quark and Antiquark Distributions

In Fig.2 we show different nuclear effects for the  $C$ -even and the  $C$ -odd isoscalar and isovector combinations of the quark distributions calculated for  $^{184}\text{W}$  and  $^2\text{H}$  nucleus.<sup>7</sup> The smearing with the nuclear spectral function (Fermi motion and nuclear binding, or FMB), the off-shell correction (OS), the nuclear coherent correction (NS), and the nuclear meson (PI) correction are treated as discussed in Sec.II. In the calculation of FMB we use a nuclear spectral function which takes into account the mean-field contribution as well as short-range nuclear correlations [15]. Note that the isoscalar and the isovector nuclear spectral functions

<sup>7</sup> Note that the light quark contributions to the isoscalar neutrino structure functions  $F_2^{\nu+\bar{\nu}}$  and  $F_3^{\nu+\bar{\nu}}$  are driven by  $q_0^+$  and  $q_0^-$ , respectively. The isovector combinations (asymmetries)  $F_2^{\nu-\bar{\nu}}$  and  $F_3^{\nu-\bar{\nu}}$  are determined by  $q_1^-$  and  $q_1^+$ , respectively.

differ significantly in Ref.[15]. The OS correction is driven by the function  $\delta f(x)$  in Eq.(6b). Note that by the definition  $\delta f$  describes relative off-shell effect in a quark distribution in an off-shell nucleon. We use the results of Ref.[15] and assume a universal OS function  $\delta f(x)$ , i.e. same function  $\delta f(x)$  for the proton and neutron and for all quark and antiquark distributions.

From the upper panel of Fig.2 we see that the FMB correction at small  $x$  has a different sign for the  $C$ -even and  $C$ -odd isoscalar distributions. This effect is due to the significantly different  $x$  dependence of  $q_0^+$  and  $q_0^-$  at low  $x$ .

At  $x < 0.01$  the NS correction for the valence quark distribution  $q_0^-$  is enhanced relative to that for  $q_0^+$ . The underlying reason for this effect is the enhancement of the multiple scattering corrections for the cross section asymmetry as discussed in Sec.II C. If we keep only the double scattering correction, then the ratio  $\delta\mathcal{R}_0^-/\delta\mathcal{R}_0^+$  is given by Eq.(35). Nevertheless, because of a partial cancellation between FMB and NS corrections for  $q_0^-$ , the magnitude of the overall relative nuclear correction at  $x < 0.01$  is similar for valence and sea quarks, being somewhat larger for the former.

Both distributions, the  $C$ -odd valence  $q_0^-$  and the  $C$ -even  $q_0^+$ , are subject to the antishadowing correction at  $x \sim 0.1$ . However, the mechanisms responsible for the antishadowing are different for  $q_0^+$  and  $q_0^-$ . The enhancement in  $q_0^+$  is due to the combined effect of the OS and PI corrections. Instead, the PI correction to  $q_0^-$  cancels out, as discussed in Sec.II B, and the enhancement in the ratio  $\mathcal{R}_0^-$  is entirely due to a constructive interference in the multiple scattering effect from  $\text{Re } a_0^-$ .

We note that different nuclear corrections on the antiquark distribution  $\bar{q}_0 = (q_0^+ - q_0^-)/2$  largely cancel out in the antishadowing region. In this context we remark that the contribution of the second term in Eq.(37b) becomes increasingly important at  $x > 0.05$ , because of the ratio  $q_0^-(x)/\bar{q}_0(x)$ . This term is negative in that region and it partially cancels a positive nuclear pion contribution. As a result, the overall nuclear correction to the antiquark distribution is small for  $0.02 < x < 0.2$ . We will discuss some implications of this effect in the context of the Drell-Yan reaction in Sec.III.

At large  $x > 0.2$  the nuclear corrections to  $q_0^+$  and  $q_0^-$  are very similar, as both distributions are dominated by the valence quarks. It should be noted that our result for the relative nuclear correction to the valence quark distribution is stable against the specific PDF set chosen in the entire region of  $x$ . Nuclear effects for sea quarks also depend weakly on the



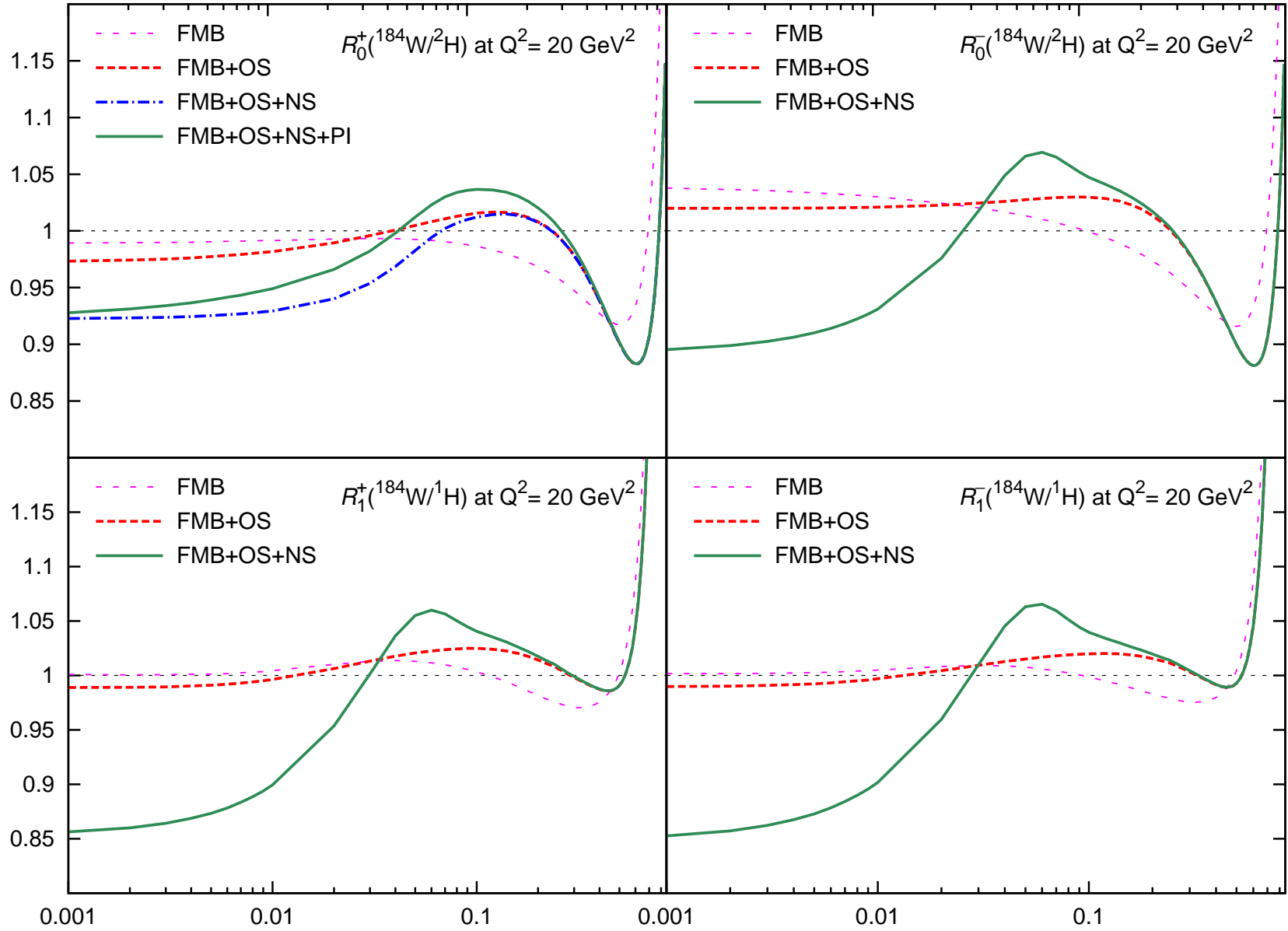


FIG. 2. Different nuclear effects on the  $C$ -even and  $C$ -odd combinations of the isoscalar  $q_0 = u + d$  (upper panel) and the isovector  $q_1 = u - d$  (lower panel) quark distributions calculated at  $Q^2 = 20 \text{ GeV}^2$ . The ratios are between  $^{184}\text{W}$  and the deuteron  $^2\text{H}$  (upper panel) and between  $^{184}\text{W}$  and the proton  $^1\text{H}$  (lower panel) (see text for details).

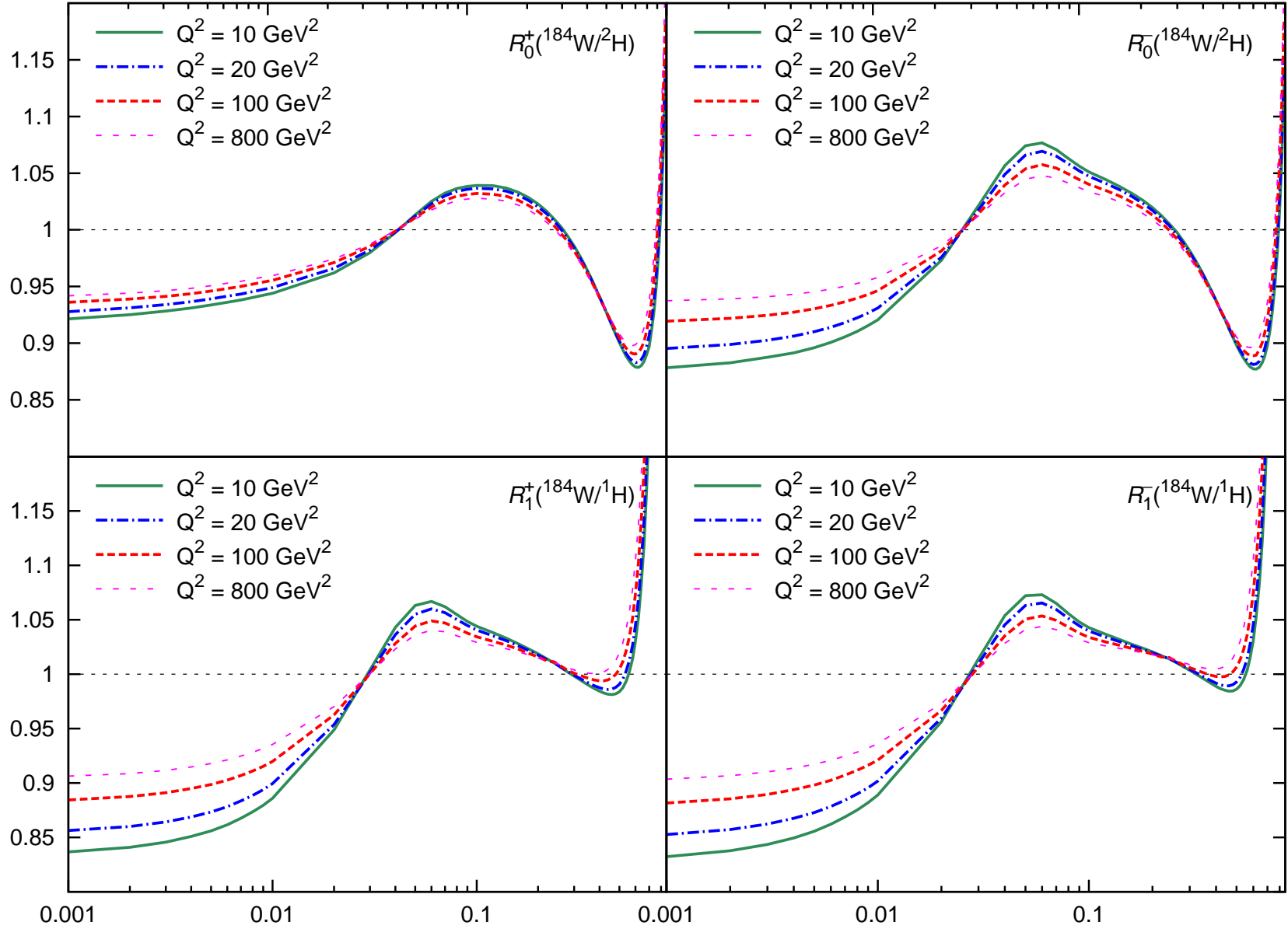


FIG. 3. The  $C$ -even and  $C$ -odd combinations of the isoscalar  $q_0 = u + d$  (upper panel) and the isovector  $q_1 = u - d$  (lower panel) quark distributions calculated at a few different  $Q^2$ . Notations are similar to those in Fig.2.

particular choice of PDF at small values of  $x$ . However, at high  $x$  the calculation of nuclear effects for antiquark distributions has larger uncertainties and the result is sensitive to both the shape and the magnitude of the nucleon antiquark distribution.

Nuclear corrections for the isovector quark distribution  $q_1 = u - d$  are shown in the lower panel of Fig.2 in the form of the ratio  $\mathcal{R}_1 = q_{1/A}/\beta q_{1/p}$ , where  $q_{1/A}$  is the nuclear distribution per one nucleon and  $q_{1/p}$  is the distribution in the proton and  $\beta = (Z - N)/A$  is fractional proton excess in a nucleus. As discussed in Sec.II the isovector nuclear distribution  $q_{1/A}$  is proportional to  $\beta$  so that  $\beta$  cancels out in the ratio  $\mathcal{R}_1$ . We observe from Fig.2 that the relative nuclear corrections for the isovector distributions  $q_1^+$  and  $q_1^-$  are similar. Furthermore the shape and the magnitude of nuclear effect at  $x < 0.1$  are similar for  $q_0^-$  and  $q_1^\pm$  and are driven by coherent nuclear correction discussed in Sec.II C. At large  $x$  the correction is dominated by the nuclear spectral function and the OS effect. There the resulting effect for the isoscalar channel differs significantly from that of the isovector channel, because of the difference between the isoscalar and the isovector nuclear spectral functions [15]. Note that the integral nuclear corrections for the valence distributions  $q_0^-$  and  $q_1^-$  are constrained by the normalization conditions Eqs. (38) and (43).

In Fig.3 we present the results on the same nuclear ratios calculated at a few different  $Q^2$ . We observe a weak  $Q^2$  dependence of nuclear effects of the  $C$ -even isoscalar  $q_0^+$ , while the  $Q^2$  dependence of other distributions is somewhat stronger.

### III. APPLICATION TO THE DRELL-YAN PROCESS

The production of lepton pairs with a large mass  $Q \gg 1$  GeV in hadron collisions occurs via the Drell-Yan process of quark-antiquark annihilation (see, e.g., [45, 46]). The corresponding cross section (Drell-Yan, or DY) depends on the product of the quark and antiquark distributions in the beam and the target:

$$\frac{d^2\sigma^{\text{DY}}}{dx_B dx_T} = K \sum_f e_f^2 [q_{f/B}(x_B, Q^2) \bar{q}_{f/T}(x_T, Q^2) + \bar{q}_{f/B}(x_B, Q^2) q_{f/T}(x_T, Q^2)], \quad (50)$$

where  $q_{f/B}$  and  $q_{f/T}$  are the quark distributions in the beam and in the target and  $e_f$  are the quark charges, respectively. The sum is taken over different quark flavors  $f$  and  $\bar{q}$  denotes the corresponding antiquark distribution. The variables measured experimentally are the mass of the lepton pair  $Q$  and the transverse and longitudinal momenta of the pair,  $k_T$

and  $k_L$  respectively. The Bjorken variables for the beam and the target,  $x_B$  and  $x_T$ , are related to these quantities as  $s x_B x_T = Q^2 + k_T^2$  with  $s$  total center-of-mass energy squared. The Feynman variable  $x_F = x_B - x_T = 2k_L/\sqrt{s}$  depends on the longitudinal momentum of the lepton pair in the center-of-mass system. The factor  $K$  in Eq.(50) absorbs kinematical factors as well as dynamical factors such as higher-order QCD corrections. In this paper we are focused on the analysis of ratios of the DY cross sections for different nuclear targets. For this reason we do not write explicitly in Eq.(50) the factors common to all targets, which are cancelling out in such ratios.

The proton-induced DY process allows a probe of antiquark distributions in the target and is complementary to the lepton-induced DIS. Indeed, in the kinematical region of large  $x_B$  and small  $x_T$  (large  $x_F$ ) the first term in Eq.(50) dominates and the ratio of the DY yields in different targets is given by the ratio of the corresponding antiquark distributions. The E772 experiment at Fermilab measured ratios of DY yields originated from the collision of a 800-GeV/ $c$  proton beam with five different nuclear targets:  $^2\text{H}$ ,  $^{12}\text{C}$ ,  $^{40}\text{Ca}$ ,  $^{56}\text{Fe}$ , and  $^{184}\text{W}$  [47]. The DY continuum was studied in the kinematic range  $4 < Q < 9$  GeV and  $Q > 11$  GeV, excluding the quarkonium region, while the Bjorken variable for the target was in the interval  $0.04 < x_T < 0.27$ . The nuclear dependence of the DY process was also measured by the E866 experiment at Fermilab, using the targets  $^9\text{Be}$ ,  $^{56}\text{Fe}$ , and  $^{184}\text{W}$  in a similar kinematic region [48].

### A. Nuclear effects on Drell-Yan cross section

The nuclear dependence of the DY process comes from two different sources: (i) the modification of the (anti)quark distributions in the target nucleus, and (ii) the initial state interaction of the projectile particle (parton) within the nuclear environment of the target. We will discuss briefly both effects in the following.

We first separate the isoscalar  $q_0$  and the isovector  $q_1$  contributions in the target in Eq.(50). We have

$$\sum_{q=u,d} e_q^2 (q_B \bar{q}_T + \bar{q}_B q_T) = \sum_{i=0,1} (p_i \bar{q}_{i/T} + \bar{p}_i q_{i/T}), \quad (51)$$

where  $p_0 = (4u + d)/18$  and  $p_1 = (4u - d)/18$  with  $u$  and  $d$  the corresponding quark distributions in the projectile and similar equations for  $\bar{p}_0$  and  $\bar{p}_1$  with the quark distributions replaced with the antiquark ones. In what follows we will discuss the contribution from the

isoscalar term. The isovector correction as well as the contributions from  $s$  and  $c$  quarks will be addressed elsewhere.

Nuclear effects on quark and antiquark distributions were discussed in Sec.II. Using those results we calculate the ratio of the DY cross sections of a heavy target and the deuteron. Figure 4 shows the results obtained at the fixed  $Q^2 = 20 \text{ GeV}^2$  and with the variables  $x_T$  and  $x_B$  bound by the relation  $s x_T x_B = Q^2$  with  $s = 1600 \text{ GeV}^2$ , corresponding to the beam energy of the E772 and E866 experiments. Note that the DY ratios in the region of small  $x_T < 0.15$  are mainly driven by the corresponding ratios of the antiquark distributions. They receive two competing contributions: (i) a positive correction due to the nuclear meson exchanged currents (see Sec.II B) and (ii) a negative correction due to nuclear shadowing (see Sec.II C). These two effects partially cancel out in the antiquark distributions. It should be noted that the shadowing correction for antiquarks extends up to a relatively large  $x_T \sim 0.1$ . This fact occurs because of the factor  $q_{val}/\bar{q}$  in Eq.(37b), which enhances the relative shadowing correction for antiquarks at increasing  $x$ . However, such an enhancement is not present for the  $q^\pm = q \pm \bar{q}$  combinations of parton distribution, as can be seen from Fig.2.

The projectile partons in the initial state can undergo multiple soft collisions and can radiate gluons before annihilating with the (anti)quarks of the target and producing a dimuon pair. Because of this effect, Eq.(50) may not be applied directly to the nuclear DY process, as we have to take into account the effects of the propagation of the projectile partons within the nuclear environment. A number of different approaches is available in literature to describe the propagation effects and the corresponding gluon radiation in the nuclear medium (for a review see, e.g., [51, 52]). However, results from different analyses significantly disagree both on the magnitude of the quark energy loss and on its energy and propagation length dependencies [52]. In this paper we follow the heuristic approach of modifying the variable  $x_B$ , in order to account for the effect of the quark energy loss [51]. Let  $E' = -dE/dz$  be the parton energy loss in a nucleus per unit length ( $E' \geq 0$ ). If a parton originated with an energy  $E_0$  travels over the distance  $L$  in the nuclear environment before annihilation, then its energy at the moment of the annihilation would be  $E_1 = E_0 - E'L$ , which will be used to create the dimuon pair. Therefore, the effect of the energy loss in the nuclear medium requires a correspondingly larger value of the initial Bjorken  $x_B$ . In our analysis we assume that Eq.(50) can be applied to the case in which a nuclear target is present with the simple replacement  $x_B \rightarrow x_B + E'L/E_B$ , where  $E_B$  is the energy of the projectile proton. Below

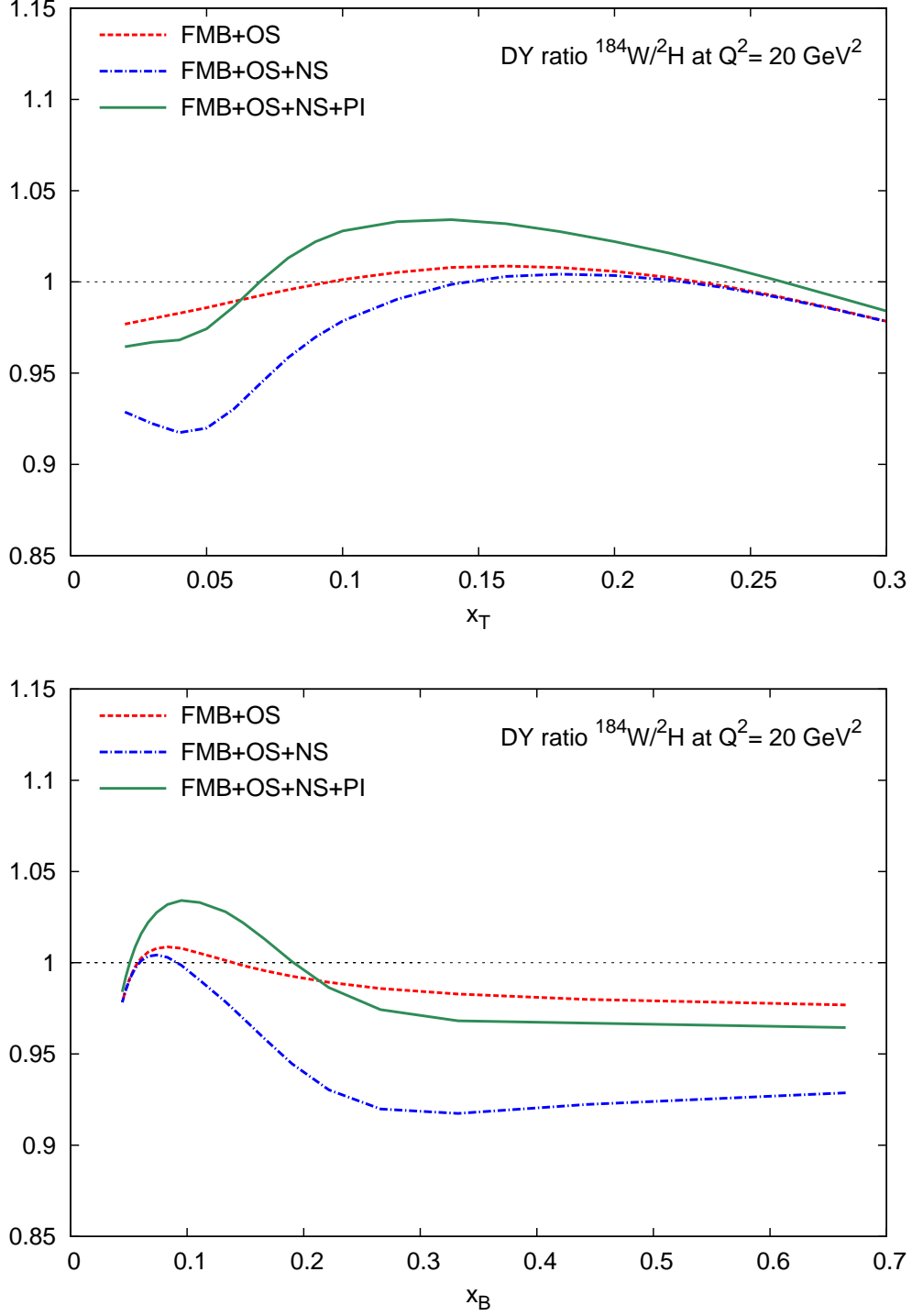


FIG. 4. Different nuclear effects on the cross section of the lepton pair production with a fixed invariant mass  $Q^2 = 20 \text{ GeV}^2$  in the collision of 800 GeV/c protons with nuclear targets. The upper panel shows the ratio of the reaction yields in Eq.(50) between tungsten  $^{184}\text{W}$  and deuterium  $^2\text{H}$  targets as a function of  $x_T$ , while the lower panel shows the same ratio as a function of  $x_B$ .

we present the results of our analysis of the combined effects originated from the nuclear modifications of the target (anti)quark distributions and from the energy loss of the beam partons in the nuclear environment. In order to check the sensitivity to the energy loss in the nuclear medium we consider a range of possible values commonly used in the literature for this latter  $0 \leq E' \leq 1.5$  GeV/fm. We estimate average propagation length in the nuclear medium of the projectile partons as  $L = 3R/4$ , which is an average distance travelled by a projectile in a uniform nuclear density distribution within a sphere of radius  $R$ .

## B. Comparison with Drell-Yan data

Figure 5 shows a comparison of our predictions with the data from the E772 experiment for a number of nuclear targets [47, 49]. Although most of the E772 data cover the kinematic region in which anti-shadowing is expected according to DIS data ( $0.1 < x < 0.3$ ), no enhancement is observed in the ratio of the DY yields for heavy nuclei and deuterium. This observation gave rise to a long standing puzzle since the nuclear binding should result in an excess of nuclear mesons, which is expected to produce a marked enhancement in the nuclear anti-quark distributions. However, in the discussed approach we found a very good agreement of our predictions with the E772 DY data, as illustrated in Fig. 5. This fact is explained by a cancellation between a positive correction due to enhancement of the nuclear meson field and a negative shadowing correction for antiquark distributions (see Sec.IIF). Finally, the lowest values of  $x_T$  in Fig.5 clearly show evidence of nuclear shadowing in the data of E772 experiment, in good agreement with the shown predictions.

It is worth noting that the good agreement observed with DY data also supports our hypothesis of a common off-shell structure function  $\delta f(x)$  for the valence and the sea quark distributions.

Figure 6 shows the E772 data as a function of  $x_B$  for various bins in the invariant mass of the dimuon pair [47, 49] together with our predictions. This representation allows a better visualization of the effect of the projectile energy loss in the nuclear medium, which is expected to increase with  $x_B$ . The solid curves represent our predictions with a fixed value  $E' = 0.7$  GeV/fm. The E772 data in both Fig.5 and 6 favor the presence of moderate energy loss effects. Overall, we obtain a very good description of E772 data for both the magnitude and the  $x$  and mass dependence of the DY cross-section ratios. We note that the

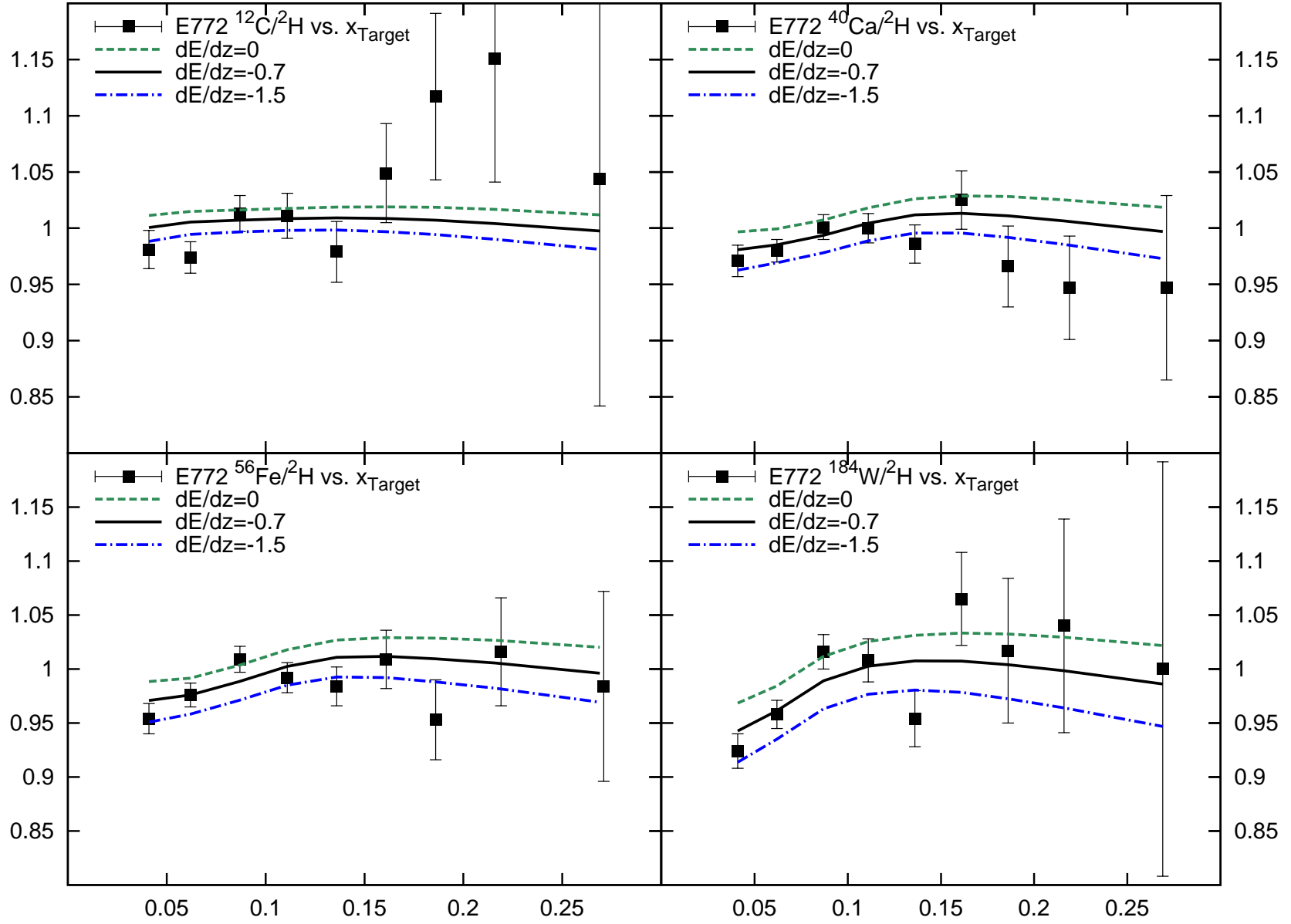


FIG. 5. Ratio of the DY reaction cross sections for different nuclei as a function of  $x_T$ . Data points are taken from the E772 experiment [47, 49], while the curves represent our predictions with (solid) and without (dashed) the energy loss correction to the projectile quark (see text for details).



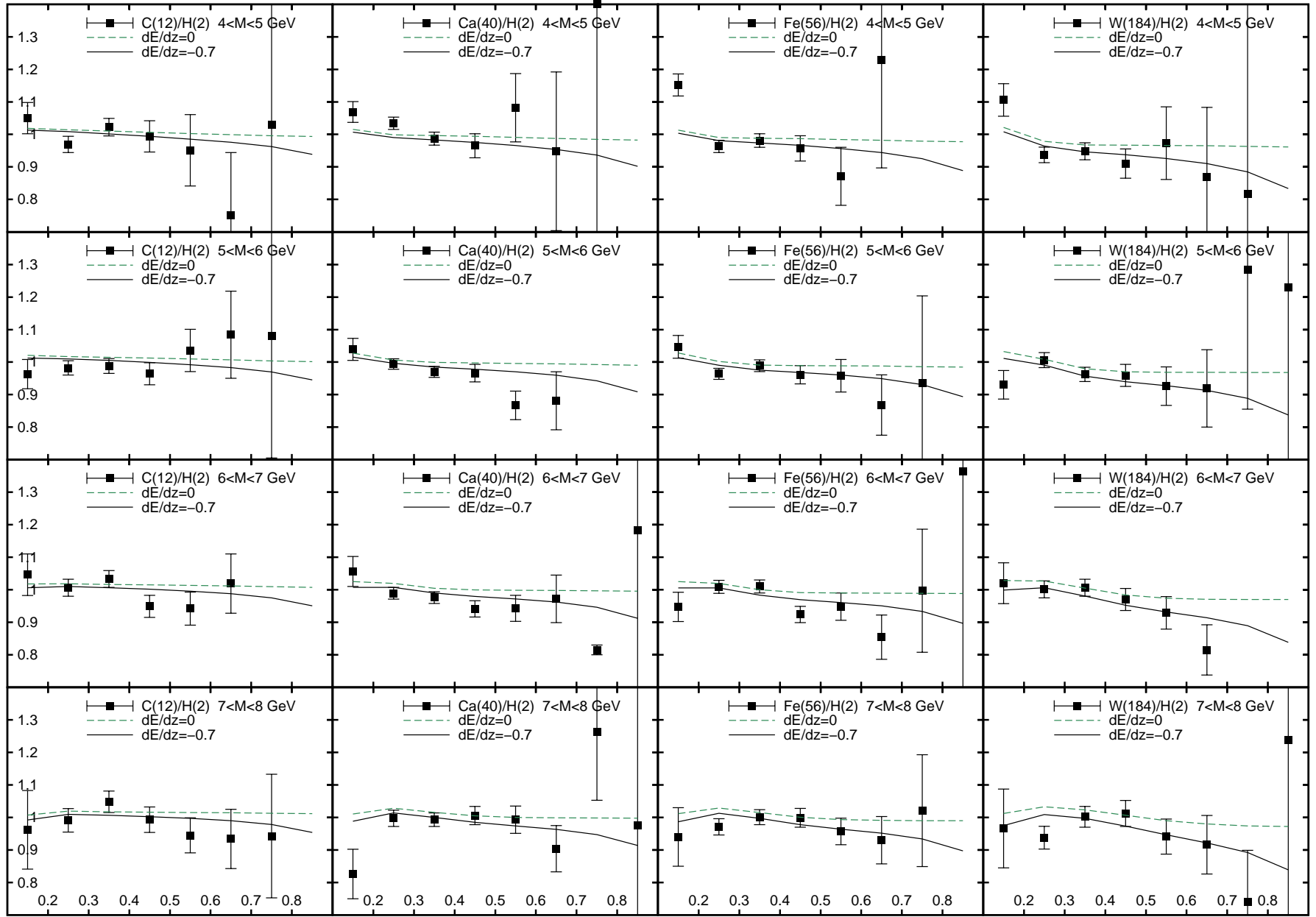


FIG. 6. Ratio of the DY reaction cross sections for different nuclei (rows) and dimuon mass bins (columns), as a function of  $x_B$ . Data points are taken from the E772 experiment [47, 49], while the curves represent our predictions with (solid) and without (dashed) the energy loss correction to the projectile quark (see text for details).

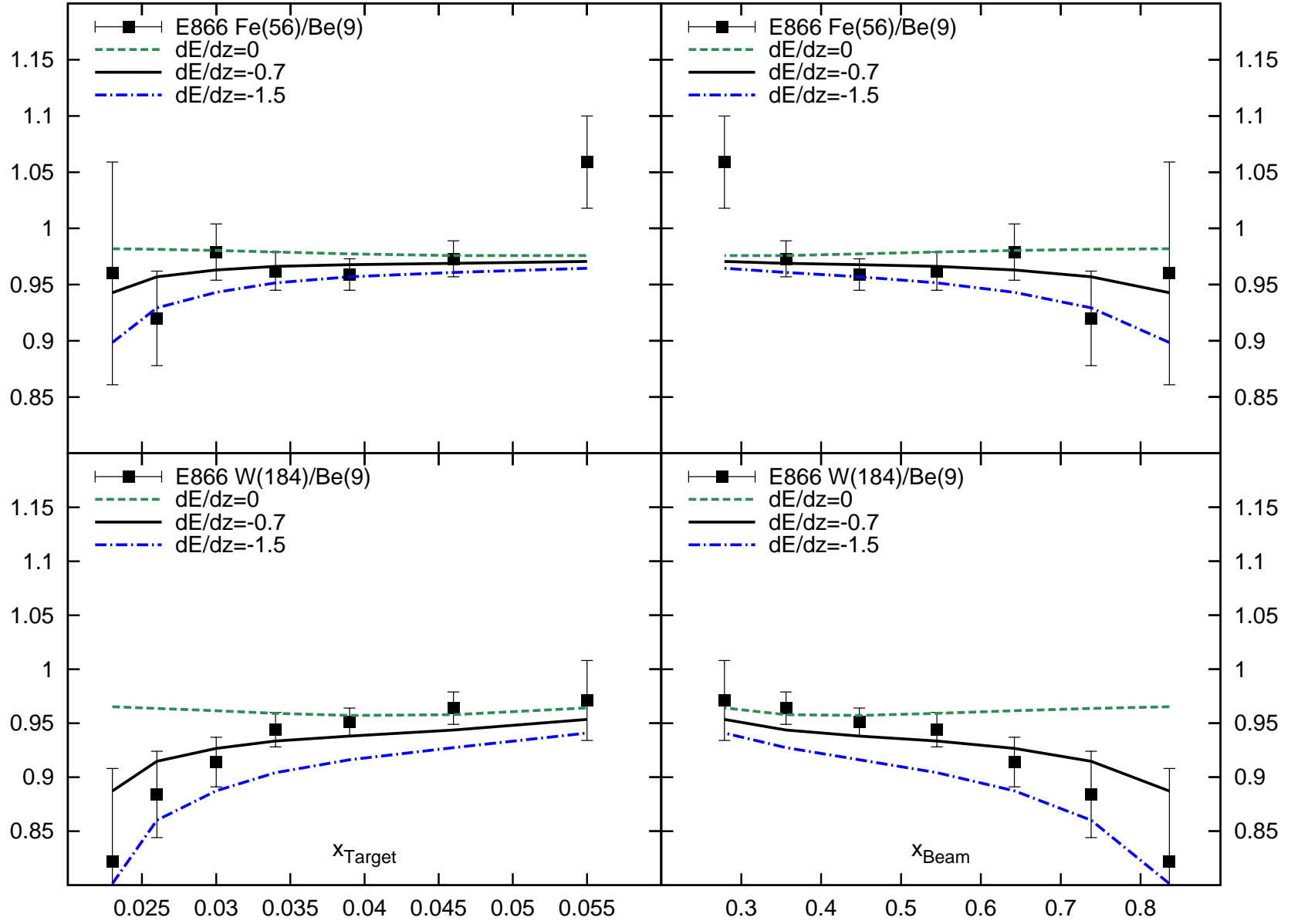


FIG. 7. Comparison of the ratio of the DY reaction yields in different nuclei from the E866 experiment [48] with our predictions with (solid) and without (dashed) the quark energy loss correction.

kinematic coverage of the E772 data is mainly focused on the region of intermediate  $x_T$  and  $x_B$  and is not optimal to address the energy loss effects nor the nuclear shadowing.

The data from the E866 experiment [48] is shifted towards lower values of  $x_T$  and higher values of  $x_B$  with respect to E772 data, as can be seen from Fig. 7. The kinematic coverage of E866 data is therefore focused on the region where both shadowing and energy loss effects become more prominent. The E866 data are consistent with the E772 data in the overlap region. Figure 7 shows that our predictions for the E866 kinematics are in good agreement with the E866 data.

We varied the parameter  $E'$  describing the parton energy loss within the interval from 0 to 1.5 GeV/fm in order to find its optimum value. To this end, we evaluated the  $\chi^2$  between our predictions and the E772 and E866 data in Figures 5 and 7. The best fit corresponds to a value  $E' = 0.70 \pm 0.15$  GeV/fm with  $\chi^2/d.o.f. = 50.8/50$ . The weights of E866 and E772 data in this analysis are comparable since the former has a higher sensitivity to energy loss effects, but the latter has more data points available. We note that there is a strong correlation in the data between the shadowing correction and the energy loss effect, due to the fixed target kinematics which correlates small values of  $x_T$  to large values of  $x_B$ . Furthermore, the kinematic coverage of available DY data is limited to regions in which both effects result in considerable corrections.

A new measurement of nuclear effects in the DY production is planned in the experiment E906 at Fermilab [53]. This experiment will be carried out with a 120 GeV proton beam and it is planned to collect about a factor of 50 larger statistics than E772 using different nuclear targets. The kinematic coverage of E906 data will extend at much larger  $x_T$  and should allow to disentangle the energy loss effect from the shadowing corrections.

#### IV. DISCUSSION

In this article we study nuclear PDFs basing on the semi-microscopic model of Ref. [15], focusing at the region of high invariant momentum transfer  $Q$ . We discussed in details the  $C$ -even and  $C$ -odd combinations of the isoscalar  $q_0 = u + d$  and the isovector  $q_1 = u - d$  distributions and found a substantial dependence of nuclear effects on both the  $C$  parity and the isospin of the parton distributions.

In the region of large  $x > 0.2$  the nuclear PDFs are dominated by incoherent contribution

of bound protons and neutrons and the nuclear corrections are driven by the nuclear spectral function effects together with off-shell correction. The slope of the ratios of the nuclear and the deuteron PDFs for  $0.3 < x < 0.6$  and their minimum around  $x \sim 0.6$  (EMC effect) are explained by a competition between nuclear binding, Fermi motion and off-shell corrections. We observe a substantial difference in the magnitude of the resulting effect for  $q_0$  and  $q_1$  as demonstrated in Fig.2, mainly due to the difference in the isoscalar and the isovector spectral functions.

All nPDFs show an antishadowing enhancement in the region  $0.03 < x < 0.3$  and a shadowing suppression at  $x < 0.03$ . However, the antishadowing effects for the  $q_0^+$  and  $q_0^-$  distributions are driven by different mechanisms. The enhancement of  $q_0^+$  is a combined effect of the off-shell and nuclear meson corrections, while the anti-shadowing of  $q_0^-$  is due to the constructive interference from the real part of the effective scattering amplitude in the nuclear multiple scattering series.

The relative correction of the nuclear shadowing is enhanced for the valence quark distributions ( $C$ -odd) and also for the isovector combinations. This effect follows from the corresponding enhancement of the propagation effects in the nuclear environment, as discussed in Section II C. We note that at small  $x$  the combined effect of the nuclear binding and Fermi motion corrections has a different sign for the  $q_0^+$  and  $q_0^-$  distributions, due to the different  $x$  dependence of those distributions. The off-shell correction is negative for  $x < 0.02$  for both distributions. We found a partial cancellation between the nuclear binding and off-shell effects in the valence quark distribution  $q_0^-$  at small  $x$ . However, both corrections are negative and somewhat enhance the shadowing effect in the  $q_0^+$  distribution. Overall, the shadowing effect for the  $q_0^-$  distribution is more pronounced. We observe a similar behavior for the isovector quark distributions  $q_1^\pm$ . We also find a weak  $Q^2$  dependence of nuclear effects of the  $C$ -even isoscalar  $q_0^+$ , while the  $Q^2$  dependence of other distributions is somewhat stronger.

The PDF normalization conditions and the energy-momentum sum rules link different nuclear effects located in different kinematical regions of  $x$ . In Sec.II D we used the normalization conditions for isoscalar and isovector valence quark distributions as dynamical equations to fix unknown amplitudes controlling the coherent nuclear correction. These equations are then solved in terms of off-shell correction to corresponding distribution. We also use the light-cone momentum sum rule to constrain the mesonic light-cone distributions

and calculate the corresponding mesonic corrections to nuclear PDFs, which is discussed in Sec.II B.

The developed model was applied to calculate the cross-sections for DY production in proton-nucleus collisions. We recapitulate that the E772 data on the ratio of DY reaction yields for different nuclear targets shows no enhancement of the nuclear sea quark distributions in the antishadowing region  $x \sim 0.05 - 0.2$ . This behavior is in contrast with predictions of enhancement of nuclear sea due to nuclear meson contribution. We found that this discrepancy can be explained by a partial cancellation between different nuclear corrections on the antiquark distributions in the "antishadowing" region  $x \sim 0.05 - 0.2$ , as discussed in Sec.II F. A detailed comparison of our predictions with data [47, 48] in Sec.III reveals a very good agreement with both the magnitude of the measured ratios and their  $x$  and dimuon mass dependence. We also discussed the impact of the energy loss of the projectile partons in the nuclear environment on the ratio of the DY yields for nuclear targets and found that our analysis favors the energy loss around 0.7 GeV/fm.

As a final remark we note that the studies of nuclear effects in the isovector combinations of (anti)quark distributions  $q_1$  are important for a correct calculation of the neutron excess effect in heavy nuclei in high-energy nuclear reactions, including DIS and DY process. Also the isovector distributions are of direct relevance for neutrino physics, as they determine the  $\nu - \bar{\nu}$  asymmetries in neutrino-nuclear collisions [16, 54, 55]. In particular, an accurate knowledge of such effects is crucial for the interpretation of data in modern neutrino experiments [56, 57]. This in turn requires the detailed studies of the isovector component of the nuclear spectral function as well as the isospin dependence of the off-shell correction  $\delta f$ .

## ACKNOWLEDGEMENTS

We thank G.A. Miller for interesting discussions on the topics covered in this work.

- 
- [1] J. C. Collins, D. E. Soper and G. F. Sterman, Adv. Ser. Direct. High Energy Phys. **5**, 1 (1988) [hep-ph/0409313].
  - [2] S. Alekhin, J. Blumlein and S. Moch, Phys. Rev. D **86**, 054009 (2012) [arXiv:1202.2281 [hep-ph]].
  - [3] A. D. Martin, W. J. Stirling, R. S. Thorne and G. Watt, Eur. Phys. J. C **63**, 189 (2009) [arXiv:0901.0002 [hep-ph]].
  - [4] R. D. Ball, V. Bertone, S. Carrazza, C. S. Deans, L. Del Debbio, S. Forte, A. Guffanti and N. P. Hartland *et al.*, Nucl. Phys. B **867**, 244 (2013) [arXiv:1207.1303 [hep-ph]].
  - [5] J. Gao, M. Guzzi, J. Huston, H. -L. Lai, Z. Li, P. Nadolsky, J. Pumplin and D. Stump *et al.*, arXiv:1302.6246 [hep-ph].
  - [6] M. Arneodo, Phys. Rept. **240**, 301-393 (1994).
  - [7] P. R. Norton, Rept. Prog. Phys. **66**, 1253 (2003).
  - [8] D. F. Geesaman, K. Saito and A. Thomas, Ann. Rev. Nucl. Part. Sci. **45**, 337-390 (1995).
  - [9] R. P. Bickerstaff and A. W. Thomas, J. Phys. G **15**, 1523 (1989).
  - [10] K. J. Eskola, H. Paukkunen and C. A. Salgado, JHEP **0904**, 065 (2009) [arXiv:0902.4154 [hep-ph]].
  - [11] M. Hirai, S. Kumano and T. -H. Nagai, Phys. Rev. C **76**, 065207 (2007) [arXiv:0709.3038 [hep-ph]].
  - [12] D. de Florian, R. Sassot, P. Zurita and M. Stratmann, Phys. Rev. D **85**, 074028 (2012) [arXiv:1112.6324 [hep-ph]].
  - [13] K. Kovarik, I. Schienbein, F. I. Olness, J. Y. Yu, C. Keppel, J. G. Morfin, J. F. Owens and T. Stavreva, Phys. Rev. Lett. **106**, 122301 (2011) [arXiv:1012.0286 [hep-ph]].
  - [14] H. Paukkunen and C. A. Salgado, Phys. Rev. Lett. **110**, no. 21, 212301 (2013) [arXiv:1302.2001 [hep-ph]].
  - [15] S. A. Kulagin and R. Petti, Nucl. Phys. A **765**, 126 (2006) [arXiv:hep-ph/0412425].
  - [16] S. A. Kulagin and R. Petti, Phys. Rev. D **76**, 094023 (2007) [arXiv:hep-ph/0703033].
  - [17] S. A. Kulagin and R. Petti, Phys. Rev. C **82**, 054614 (2010) [arXiv:1004.3062 [hep-ph]].
  - [18] S. V. Akulinichev, S. A. Kulagin and G. M. Vagradov, Phys. Lett. B **158**, 485 (1985).

- [19] S. V. Akulinichev, G. M. Vagradov and S. A. Kulagin, JETP Lett. **42**, 127 (1985) [Pisma Zh. Eksp. Teor. Fiz. **42**, 105 (1985)].
- [20] S. V. Akulinichev, S. Shlomo, S. A. Kulagin and G. M. Vagradov, Phys. Rev. Lett. **55**, 2239 (1985).
- [21] S. A. Kulagin, Nucl. Phys. A **500**, 653 (1989).
- [22] S. A. Kulagin, G. Piller and W. Weise, Phys. Rev. C **50**, 1154 (1994) [nucl-th/9402015].
- [23] S. A. Kulagin and W. Melnitchouk, Phys. Rev. C **78**, 065203 (2008) [arXiv:0809.3998 [nucl-th]].
- [24] T. H. Bauer, R. D. Spital, D. R. Yennie and F. M. Pipkin, Rev. Mod. Phys. **50**, 261 (1978) [Erratum-ibid. **51**, 407 (1979)].
- [25] N. N. Nikolaev and B. G. Zakharov, Z. Phys. C **49**, 607 (1991).
- [26] G. Piller and W. Weise, Phys. Rept. **330**, 1 (2000) [hep-ph/9908230].
- [27] R. J. Glauber, Phys. Rev. **100**, 242 (1955).
- [28] V. N. Gribov, Sov. Phys. JETP **30**, 709 (1970) [Zh. Eksp. Teor. Fiz. **57**, 1306 (1969)].
- [29] N. N. Nikolaev and V. I. Zakharov, Phys. Lett. B **55**, 397 (1975).
- [30] L. L. Frankfurt, M. I. Strikman and S. Liuti, Phys. Rev. Lett. **65**, 1725 (1990).
- [31] B. L. Ioffe, V. A. Khoze and L. N. Lipatov, “Hard Processes. Vol. 1: Phenomenology, Quark Parton Model,” Amsterdam, Netherlands: North-holland (1984) 340p
- [32] S. A. Kulagin, arXiv:hep-ph/9812532.
- [33] C. H. Llewellyn Smith, Phys. Lett. B **128**, 107 (1983);
- [34] M. Ericson and A. W. Thomas, Phys. Lett. B **128**, 112 (1983);
- [35] E. L. Berger and F. Coester, Phys. Rev. D **32**, 1071 (1985);
- [36] B. L. Friman, V. R. Pandharipande and R. B. Wiringa, Phys. Rev. Lett. **51**, 763 (1983);
- [37] E. E. Sapershtein and M. Z. Shmatikov, JETP Lett. **41**, 53 (1985) [Pisma Zh. Eksp. Teor. Fiz. **41**, 44 (1985)];
- [38] L. P. Kaptari, A. I. Titov, E. L. Bratkovskaya and A. Y. Umnikov, Nucl. Phys. A **512**, 684 (1990);
- [39] H. Jung and G. A. Miller, Phys. Rev. C **41**, 659 (1990);
- [40] D. S. Koltun, Phys. Rev. C **57**, 1210 (1998) [arXiv:nucl-th/9709033].
- [41] C. L. Korpa and A. E. L. Dieperink, Phys. Rev. C **87**, 014616 (2013) [arXiv:1301.2463 [nucl-th]].

- [42] S. Alekhin, K. Melnikov and F. Petriello, Phys. Rev. D **74**, 054033 (2006) [hep-ph/0606237].
- [43] S. Alekhin, S. A. Kulagin and R. Petti, AIP Conf. Proc. **967**, 215 (2007) [arXiv:0710.0124 [hep-ph]].
- [44] R. P. Bickerstaff, M. C. Birse and G. A. Miller, Phys. Rev. Lett. **53**, 2532 (1984).
- [45] P. L. McGaughey, J. M. Moss and J. C. Peng, Ann. Rev. Nucl. Part. Sci. **49**, 217 (1999) [hep-ph/9905409].
- [46] J. -C. Peng and J. -W. Qiu, arXiv:1401.0934 [hep-ph].
- [47] D. M. Alde *et al.*, Phys. Rev. Lett. **64**, 2479 (1990).
- [48] M. A. Vasilev *et al.* [FNAL E866 and NuSea Collaborations], Phys. Rev. Lett. **83**, 2304 (1999) [hep-ex/9906010].
- [49] E866/E789/E772 web resources <http://p25ext.lanl.gov/e866/papers/papers.html>
- [50] J. T. Londergan, J. C. Peng and A. W. Thomas, Rev. Mod. Phys. **82**, 2009 (2010) [arXiv:0907.2352 [hep-ph]].
- [51] G. T. Garvey and J. C. Peng, Phys. Rev. Lett. **90**, 092302 (2003) [hep-ph/0208145].
- [52] A. Accardi, F. Arleo, W. K. Brooks, D. D’Enterria and V. Muccifora, Riv. Nuovo Cim. **32**, 439 (2010) [arXiv:0907.3534 [nucl-th]].
- [53] J. Arrington, *et al.* [E906 Collaboration], Fermilab Projects-doc-395, 2006, <http://projects-docdb.fnal.gov/cgi-bin/ShowDocument?docid=395>; P. E. Reimer, Eur. Phys. J. A **31**, 593 (2007); P. E. Reimer [Fermilab SeaQuest Collaboration], J. Phys. Conf. Ser. **295**, 012011 (2011).
- [54] S. A. Kulagin, Phys. Rev. D **67**, 091301 (2003) [arXiv:hep-ph/0301045];
- [55] S. A. Kulagin, Nucl. Phys. Proc. Suppl. **139**, 213 (2005) [arXiv:hep-ph/0409057].
- [56] S. R. Mishra, R. Petti and C. Rosenfeld, PoS NUFACT **08**, 069 (2008) [arXiv:0812.4527 [hep-ex]].
- [57] C. Adams *et al.* [LBNE Collaboration], arXiv:1307.7335 [hep-ex].